



The putative myristoylome of *Physcomitrium patens* reveals conserved features of myristylation in basal land plants

Linyu Lai¹ · Jingtong Ruan¹ · Chaowen Xiao¹ · Peishan Yi¹

Received: 8 February 2023 / Accepted: 3 April 2023 / Published online: 13 April 2023
© The Author(s), under exclusive licence to Springer-Verlag GmbH Germany, part of Springer Nature 2023

Abstract

Key message The putative myristoylome of moss *P. patens* opens an avenue for studying myristylation substrates in non-canonical model plants. A myristylation signal was shown sufficient for membrane targeting and useful for membrane dynamics visualization during cell growth.

Abstract *N*-myristylation (MYR) is one form of lipid modification catalyzed by *N*-myristoyltransferase that enables protein-membrane association. MYR is highly conserved in all eukaryotes. However, the study of MYR is limited to a few models such as yeasts, humans, and Arabidopsis. Here, using prediction tools, we report the characterization of the putative myristoylome of the moss *Physcomitrium patens*. We show that basal land plants display a similar signature of MYR to Arabidopsis and may have organism-specific substrates. Phylogenetically, MYR signals have mostly co-evolved with protein function but also exhibit variability in an organism-specific manner. We also demonstrate that the MYR motif of a moss brassinosteroid-signaling kinase is an efficient plasma membrane targeting signal and labels lipid-rich domains in tip-growing cells. Our results provide insights into the myristoylome in a basal land plant and lay the foundation for future studies on MYR and its roles in plant evolution.

Keywords Myristylation · *Physcomitrium patens* · Plasma membrane · Calcium-dependent protein kinase · Calcineurin B-like protein · Brassinosteroid-signaling kinase · Tip growth

Introduction

N-terminal myristylation (MYR) is one of the main eukaryotic protein modifications (Ramazi and Zahiri 2021). MYR occurs cotranslationally (Wilcox et al. 1987) and is catalyzed by *N*-myristoyltransferase (NMT) that transfers the myristoyl moiety to Glycine 2 (Gly2) after the removal of the methionine initiator of a target protein (Towler et al. 1987; Boisson et al. 2003; Meinnel et al. 2020). MYR functions primarily to anchor proteins to membranes through interactions between the myristoyl group and membrane lipids (Giglione and Meinnel 2021). Thus, many myristoylated

(MYRed) proteins localize at the plasma membrane (PM) and membranous organelles such as endoplasmic reticulum, endosome, Golgi, and vacuole (Meinnel et al. 2020). MYR is generally considered insufficient for membrane targeting (Giglione and Meinnel 2021). A strong membrane association requires additional signals such as S-palmitoylation on the vicinal cysteines of Gly2 (Solis et al. 2022) and/or electrostatic interactions involving positively charged residues (Xiong et al. 2021). For this reason, many MYRed proteins shuttle between membrane compartments (Giglione and Meinnel 2021).

The identification of MYRed proteins has been central to understanding myristylation mechanisms and their functional relevance. Using mass spectrometry and in vitro enzymatic assays, early studies in unicellular organisms (Ashrafi et al. 1998; Traverso et al. 2013), humans (Thinon et al. 2014), and Arabidopsis (Boisson et al. 2003; Pierre et al. 2007; Martinez et al. 2008; Yamauchi et al. 2010) have revealed a myriad of MYRed proteins. Recently, the near-complete myristoylomes of humans and Arabidopsis have been characterized (Castrec et al. 2018; Majeran et al. 2018).

Communicated by Xian Sheng Zhang.

✉ Peishan Yi
yipeishan@scu.edu.cn

¹ Key Laboratory of Bio-Resource and Eco-Environment of Ministry of Education, College of Life Sciences, Sichuan University, No. 24 South Section 1, Yihuan Road, Wuhou District, Chengdu, Sichuan 610064, People's Republic of China

These studies uncover the presence of ~2% MYRed proteins in each organism and a linear correlation between the proteome and myristoylome sizes (Meinnel et al. 2020). Importantly, a subset of MYRed proteins are differentially associated with membrane compartments in all studied eukaryotes (Meinnel et al. 2020). These facts, along with structural similarities between NMTs and prokaryotic GCN5-related N-acetyltransferases (Bhatnagar et al. 1998; Thimon et al. 2014), suggest that MYR and its substrates play critical roles in membrane compartmentalization during eukaryogenesis (Meinnel et al. 2020).

To date, studies of MYR in plants are limited to Arabidopsis. In the Arabidopsis genome, two NMTs are initially identified, but only AtNMT1 is catalytically similar to yeast and human NMTs (Qi et al. 2000). AtNMT2 is considered a pseudogene because there is a one-base deletion in the open reading frame (<https://www.arabidopsis.org>). Moreover, AtNMT2 is poorly expressed and is neither biochemically active (Boisson et al. 2003) nor required for development (Pierre et al. 2007). AtNMT1 is functionally interchangeable with human HsNMT1/2 (Qi et al. 2000; Pierre et al. 2007) and exhibits similar substrate specificities (Martinez et al. 2008; Traverso et al. 2013; Castrec et al. 2018). By contrast, yeast ScNMT1 cannot complement the loss of AtNMT1 (Boisson et al. 2003; Pierre et al. 2007) and is more stringent on substrate selection (Traverso et al. 2013). Crystal structures of HsNMT1 and ScNMT1 have revealed significant conformational differences for substrate binding (Bhatnagar et al. 1998; Thimon et al. 2014; Castrec et al. 2018). Therefore, NMTs are diverged in early eukaryotes and may impact distinct signaling events in different eukaryotic lineages and pathways, yet whether it is true remains elusive.

Previous in vitro and proteomics studies have identified hundreds of MYRed substrates in human and Arabidopsis (Boisson et al. 2003; Martinez et al. 2008; Yamauchi et al. 2010; Thimon et al. 2014; Castrec et al. 2018; Majeran et al. 2018). This leads to the characterization of sequence consensus at the N-termini of MYRed proteins. Briefly, MYR depends on a specific glycine at position 2 and is favored by serine at position 6; residues at position 3–5 tend to be small and non-charged; position 7 is preferentially a positively charged residue (Meinnel et al. 2020; Giglione and Meinnel 2021). The available information along with in-silicon training has enabled the development of computational tools that predict MYRed proteins (Maurer-Stroh et al. 2002; Bologna et al. 2004; Podell and Gribskov 2004; Martinez et al. 2008; Madeo et al. 2022).

In this study, we use computational tools combined with homology analyses to predict MYRed proteins in the early diverging land plant *Physcomitrium patens* (*P. patens*). We identify 761 putative MYR targets, of which 14% are of high confidence. MYR substrate candidates are enriched in protein phosphorylation, protein degradation, and signaling

transduction pathways and comprise bryophyte-specific genes. Phylogenetically, MYR signals are clustered in protein subgroups and can emerge or lose in a few members. Our results provide a first glance at the putative myristoylome in a basal land plant and lay the foundation for future studies on MYR and its roles in plant evolution.

Results

Land plant N-myristoyltransferase originates from a diverged ancestor in green algae

To gain insight into the myristoylome of basal land plants, we first asked how NMTs of bryophytes, the extant early diverging land plants comprising mosses, liverworts, and hornworts, have diverged from other NMTs of the main eukaryotic lineages. As shown in Fig. 1A, most plants and non-vertebrate animals have only one NMT. There are two copies of NMTs in the moss *P. patens* and vertebrates. Phylogenetically, the two NMTs in vertebrates are clustered into distinct subgroups, while PpNMT1 and PpNMT2 are almost identical (>90% identity). Thus, unlike vertebrate NMTs, which have evolved separately, mosses may have duplicated NMT as a result of whole genome duplication (Rensing et al. 2008). In the entire eukaryotic lineage, NMTs fall into major groups corresponding to fungi, plants, and animals (Fig. 1A) in line with previous reports (Boisson et al. 2003; Meinnel et al. 2020; Giglione and Meinnel 2021). Interestingly, NMTs from red algae (*Porphyra umbilicalis* PuNMT1) and unicellular green algae (*Chlamydomonas reinhardtii* CrNMT1) are positioned close to yeasts (Fig. 1A), while the land plant clade is more related to multicellular green algae (*Chara braunii*). These observations suggest that land plant NMTs originate from a diverged ancestor in green algae.

The crystal structures of yeast NMT1 and human NMT1/2 have been resolved (Bhatnagar et al. 1998; Wu et al. 2007; Thimon et al. 2014; Castrec et al. 2018; Dian et al. 2020; Kosciuk et al. 2020). There is no available structure of any plant NMTs. The predicted structures of *P. patens* PpNMT1 and Arabidopsis AtNMT1 by AlphaFold2 (Jumper et al. 2021) display a nearly identical architecture with HsNMT1 (Fig. 1B). The N-terminal ends of PpNMT1 and AtNMT1 fold into a putative α -helix. Although the corresponding region is not conserved (Figure S1), the majority of other NMTs are also predicted to adopt a helical structure (Jumper et al. 2021) and such a structure has been experimentally observed in ScNMT1 (Wu et al. 2007). This region is functionally involved in ribosome-binding but not catalytic activity (Glover et al. 1997). Compared to other NMTs, the yeast ScNMT1 has three uniquely extended regions in the α H, α G- β j-joining loop, and C-terminal tail (Fig. 1B and Figure S1). This difference may account for the small number

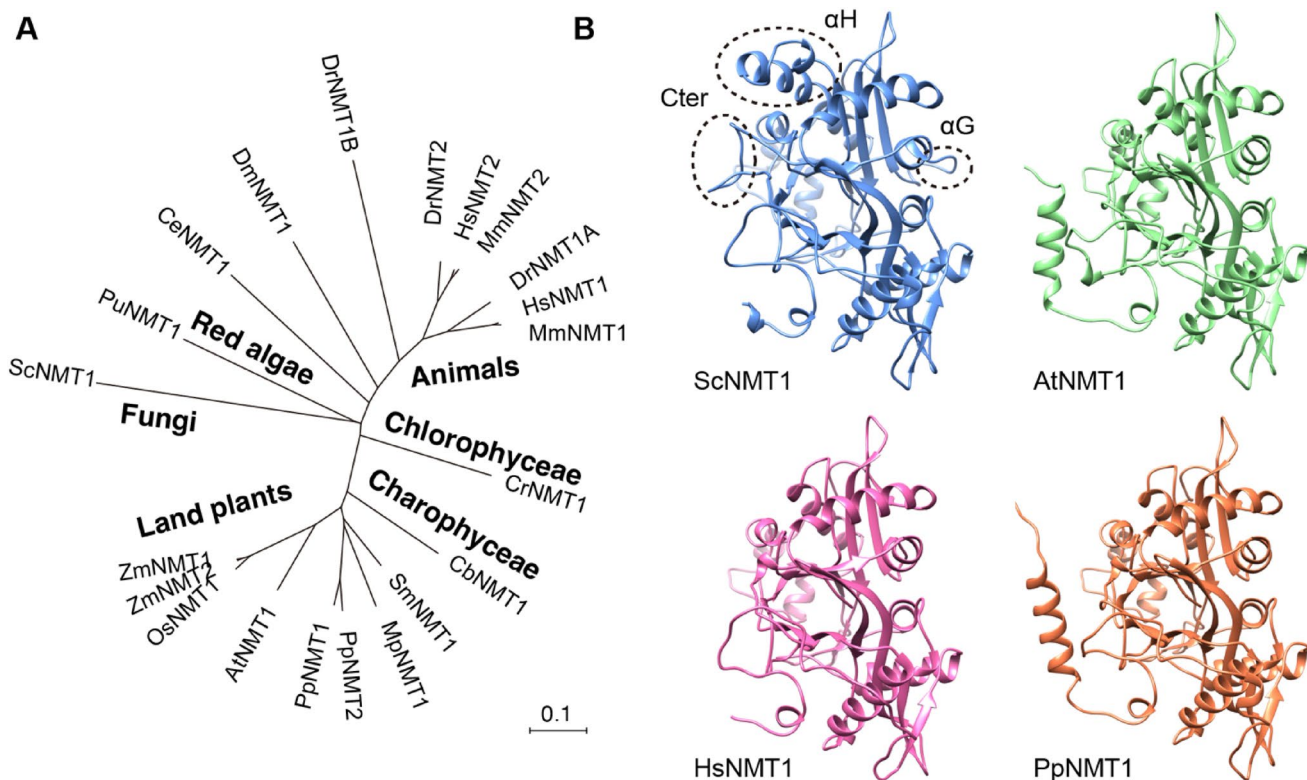


Fig. 1 Phylogenetic and structural analyses of land plant NMTs. **A** Phylogenetic tree of NMTs from selected eukaryotic lineages. Protein sequences from organisms representing fungi (*Saccharomyces cerevisiae*), red algae (*Porphyra umbilicalis*), green algae Chlorophyceae (*Chlamydomonas reinhardtii*) and Charophyceae (*Chara braunii*), animals (*Caenorhabditis elegans*, *Drosophila melanogaster*, *Danio rerio*, *Mus musculus*, and *Homo sapiens*), bryophyte mosses (*Physcomitrium patens*) and liverworts (*Marchantia polymorpha*), and vascular plants (*Selaginella moellendorffii*, *Arabidopsis thaliana*, *Oryza sativa* subsp. *japonica*, and *Zea mays*) are used to construct the

neighbor-joining tree with a bootstrap value of 1000. **B** Comparison of AlphaFold2 predicted structures of moss PpNMT1 (AF-A0A7I-4ETA1-F1) and Arabidopsis AtNMT1 (AF-Q9LTR9-F1) with crystal structures of human HsNMT1 (PDB:4C2Y) and yeast ScNMT1 (PDB:2NMT). The predicted structures display a very similar architecture to HsNMT1. Dashed circles indicate major differences in ScNMT1 and HsNMT1. ScNMT1 has extended regions in the α H, the loop between α G and β j, and the C-terminal tail. Most NMTs are predicted to have an α -helix at the N-terminal region although the corresponding sequences are not conserved (Figure S1)

of substrates (Ashrafi et al. 1998; Meinnel et al. 2020) in yeasts and the inability of ScNMT1 to rescue *Arabidopsis nmt1* mutants (Pierre et al. 2007). Interestingly, AtNMT1 and HsNMT1 could complement *ScNMT1* loss-of-function (Duronio et al. 1992; Boisson et al. 2003), implying that more NMT substrates in plants and animals have emerged. Given the similarities in function (Pierre et al. 2007), substrate specificity (Martinez et al. 2008; Traverso et al. 2013; Castrec et al. 2018), and structures (Thinon et al. 2014; Castrec et al. 2018) (Fig. 1B and Figure S1), NMTs in land plants and animals are supposed to largely retain the same enzymatic activities.

Putative myristoylome of the moss *P. patens*

Because NMTs are highly conserved in plants and animals, we suppose that prediction tools, which are mostly developed based on substrates of AtNMT1 and HsNMT1/2, could

be applied to identifying putative MYRed proteins in *P. patens*. There are four MYR-specific prediction tools: PROSITE motif and structure-guided NMT predictor (Maurer-Stroh et al. 2002), plant-optimized PlantsP (Podell and Gribskov 2004), neural network-trained Expasy myristoylator (Bologna et al. 2004), and recently developed SVMYr based on support vector machine (Madeo et al. 2022). Two additional tools, the N-terminal modification prediction tool Terminator3 (Martinez et al. 2008) and the lipid modification prediction tool GPS-lipid (Xie et al. 2016), also predict MYR substrates. To estimate the accuracy of each tool, we first predicted MYRed proteins in *Arabidopsis* and compared the results with the experimentally characterized myristoylome (Castrec et al. 2018; Majeran et al. 2018). NMT predictor, Expasy, PlantsP, and SVMYr identified 371, 488, 319, and 495 non-redundant proteins, respectively, which are comparable to the complete myristoylome (529 MYRed targets) (Castrec et al. 2018). 85, 64, 85, and 84% of the predicted

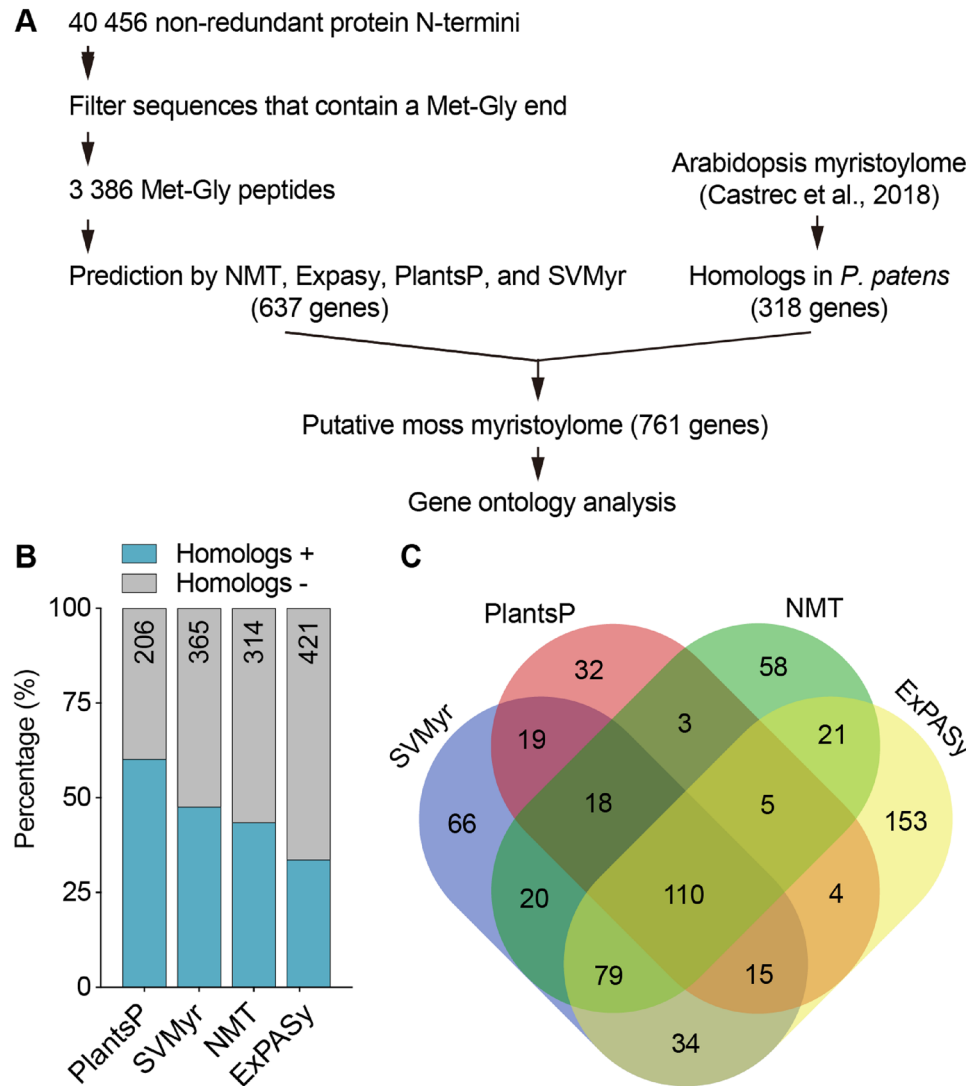
proteins in each group were present in the myristoylome (Castrec et al. 2018), suggesting a high accuracy of prediction. By contrast, Terminator3 and GPS-lipid yielded more than 1000 positive hits as a result of less stringent prediction criteria (Martinez et al. 2008; Xie et al. 2016).

Based on the performance, we used the NMT predictor, Expasy, PlantsP, and SVMYr to predict MYRed proteins in *P. patens*. The *P. patens* genome comprises 32 926 protein-coding genes that encode 87 533 protein isoforms. We extracted the N-terminal 30 amino acids (aa) of each isoform and obtained 40 456 non-redundant peptides. 3 386 of the peptides containing a Met-Gly (MG) terminus were used for prediction. Consequently, 637 genes were predicted to encode MYRed proteins by at least one method, being ~ 1.9% of the moss genome (Fig. 2A). This observation is consistent with a ~ 2% ratio of myristoylome to proteome size in other organisms (Meinnel et al. 2020), implying that the predicted myristoylome may be near complete. To make

the predicted myristoylome more inclusive, we identified genes homologous to those in the Arabidopsis myristoylome (Castrec et al. 2018). Genes encoding MG-starting peptides were added, resulting in a moss myristoylome comprising 761 genes (Table S1). Interestingly, our homology analyses revealed 983 moss genes homologous to the Arabidopsis myristoylome components. Only 318 of them (32%) encode MG-starting peptides, suggesting that MYR signals undergo substantial gain or loss during plant evolution. Accordingly, only 30% (194/637) of predicted targets have MYRed homologs in Arabidopsis.

We next compared the performance of each prediction tool. As shown in Fig. 2B, 60% (124/206), 48% (174/365), 44% (137/314), and 34% (142/421) of the predicted MYRed proteins by PlantsP, SVMYr, NMT predictor, and Expasy, respectively, were found to have a homolog in the Arabidopsis myristoylome. Thus, PlantsP outperformed other tools. However, this is probably due to more stringent prediction

Fig. 2 Prediction of moss myristoylome. **A** Overview of the prediction workflow. Genes predicted to encode MYRed proteins by at least one of the four tools (NMT predictor, Expasy, PlantsP, and SVMYr) were pooled with *P. patens* homologs of Arabidopsis myristoylome components to generate the final putative moss myristoylome. **B** Performance comparison of each tool. Percentages of hits that have or do not have homologs in the Arabidopsis myristoylome are shown in blue and grey, respectively. The total number of hits is shown at the top. **C** Venn diagram of hit distribution (colour figure online)



criteria because PlantsP generated a much smaller set of positive hits. Nevertheless, there are 110 genes predicted by all of the four tools (Fig. 2C), which represent putative MYRed proteins with the highest confidence.

Moss MYR substrate candidates mainly associate with protein phosphorylation, protein degradation, and signaling transduction

To gain insight into the functional relevance of the putative moss myristoylome, we performed sequence and gene

ontology (GO) analyses. The moss genome contains abundant short peptide-coding genes: ~20% of genes encode peptides less than 100 aa and ~40% encode peptides less than 200 aa (Fig. 3A). Sequences of putative MYR substrates display an average length of 453 aa, which is longer than that of the entire proteome (378 aa). Additionally, MYR substrate length is almost evenly distributed ranging from 100 to 600 aa (Fig. 3A). Thus, we concluded that there is no correlation between MYR and protein size in mosses.

We next performed GO analyses. In total, 78% of the 761 putative MYR substrates were successfully mapped to

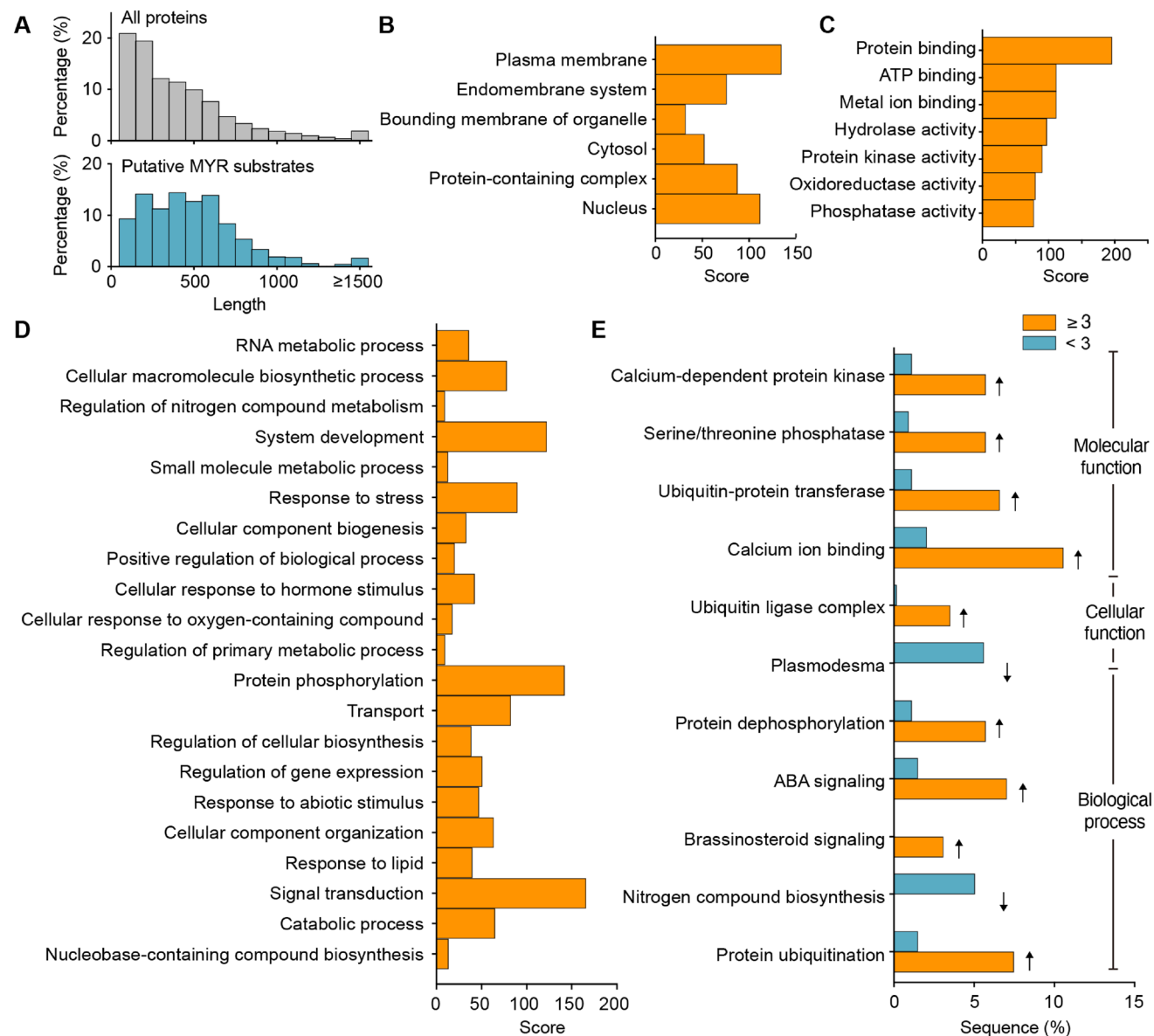


Fig. 3 Gene ontology analyses of the putative moss myristoylome. **A** Sequence length distribution of the entire proteome (grey) and putative myristoylome (blue). **B–D** The cellular function (**B**), molecular function (**C**), and biological process (**D**) enrichment of the putative

myristoylome. **(E)** GO term enrichment in predicted MYR substrates with high confidence. Percentages of sequences identified by ≥ 3 and < 3 methods are shown in orange and blue, respectively (colour figure online)

GO terms. Expectedly, the majority of the annotated genes were found to associate with the membrane (Fig. 3B). A significant number of genes were also present in protein complexes or nuclei. At the molecular function level, annotated genes were mostly enriched for protein binding and catalytic activities involving protein modification and metabolism (Fig. 3C). Accordingly, protein phosphorylation and signal transduction were the most relevant biological processes that might be regulated (Fig. 3D). As our predicted myristoylome includes 124 genes that were identified only by homology analysis and the prediction tools are not 100% accurate, there could be false-positive hits. We suppose that MYR substrates predicted by at least three methods will be of high confidence. Thus, we performed GO enrichment analysis by comparing genes predicted by ≥ 3 and < 3 tools to identify the relevant GO terms more robustly. As shown in Fig. 3E, predicted MYR substrates of high confidence are particularly enriched in calcium-binding proteins, kinases, phosphatases, and ubiquitin-related complexes, and function in protein degradation and hormone signalings. This feature appears to be conserved in land plants as a high content of kinases and calcium signaling proteins has been observed in the *Arabidopsis* myristoylome (Castrec et al. 2018; Majeran et al. 2018; Giglione and Meinnel 2021). In *Arabidopsis*, these proteins mainly localize to the PM and involve a common S-acylation on cysteines following Gly2 (Saito et al. 2018). Consistent with this notion, cysteines are highly represented in the binding motif of *Arabidopsis* MYR substrates, which is absent in animals (Castrec et al. 2018). In our prediction list, 51 and 40% of hits identified by four and three methods, respectively, also contain at least one cysteine at position 3–6. Thus, dual lipid modification appears to be common in land plants.

MYR signals during land plant evolution

We next asked how MYR signals may have changed in the plant lineage. We focused on genes with the highest probability of MYR. Among the 110 putative targets predicted by four methods, 69% have homologs in the *Arabidopsis* myristoylome (Table S2). Our BLAST results ($E\text{-value} < 10^{-20}$) additionally identified *Arabidopsis* homologs for 47% of the remaining genes (15% of the entire set). However, almost all of them have lost the critical Gly2. Finally, the last 16% of putative targets are moss or bryophyte-specific and have no closely-related homologs in *Arabidopsis* and other plants based on homology analyses in Phytozome. These data suggest that MYR signals have largely co-evolved with protein function but also emerge or lose at a discernable rate during evolution.

Land plant-specific BRO1-like proteins

To further test this possibility, we performed sequence analyses of selected MYR substrates. We first focused on membrane-associated proteins BRO1-like, Arf GTPase, and Rab GTPase, which have been predicted to undergo MYR. We identified six BRO1-like proteins. BRO1 is an endosome-associated protein initially identified in yeasts that functions in multivesicular body (MVB) formation and vacuolar protein sorting (Odorizzi et al. 2003). BRO1-like (BRO1L) proteins contain a BRO1 domain but lack the C-terminal Alix V-domain in BRO1. Our BLAST analyses identified BRO1L homologs in land plants but not in yeasts, algae, or humans, indicating that BRO1L is a land plant-specific family. Phylogenetically, BRO1L proteins cluster into four groups we named BRO1L-a to BRO1L-d (Fig. 4). Group a to c contain a highly conserved dual lipidation motif (MGCXXS) at the N-terminus. In *Arabidopsis*, it has been reported that AtBRO1L-b/BRAF localizes to the PM and MVB, and the PM localization depends on the S-acylation of Cys3 (Shen et al. 2018). AtBRO1L-b/BRAF is MYRed in vitro (Castrec et al. 2018). As S-acylation of Cys3 requires the preceding MYR (Giglione and Meinnel 2021), MYR may be essential for AtBRO1L-b/BRAF PM localization, yet this has not been experimentally examined. Compared with group a-c, group d is more closely related to human HsBROX and the BRO1 clade. Both BRO1L-d and BRO1 lack the MYR signal. These findings indicate that BRO1L-a-c together with their MYR signals have originated from a BRO1-like gene in the land plant ancestor.

Arf and Rab GTPases

Arf and Rab GTPase families each comprise a large number of members that are lipid-modified and regulate membrane trafficking. The *Arabidopsis* genome encodes 21 SAR1/ARF proteins, which fall into eight groups (Nielsen 2020). Based on homology analyses, we identified 34 members in *P. patens*, of which 21 are predicted to be MYRed by at least one method. Moss ARFs organize into nine groups with one additional moss-specific orphan group (Fig. 5). The N-terminal ends of all members of ARFA to ARFD contain Gly and Lys/Arg at position 2 and 7, respectively, which favors MYR. Indeed, they are all MYRed in *Arabidopsis* (Boisson et al. 2003; Castrec et al. 2018). Interestingly, AtARFA1 and AtARFB1 are localized to Golgi and PM, respectively, and their N-termini are necessary but not sufficient for membrane association (Matheson et al. 2008). This is likely due to the lack of Ser at position 6 and the enrichment of large hydrophobic amino acids at position 3–9. Unlike ARFs, SARA does not have putative MYR motifs. However, some ARLs could be MYRed in vitro such as AtARLC1 (Castrec et al. 2018) and are predicted to be MYRed in *P. patens*.

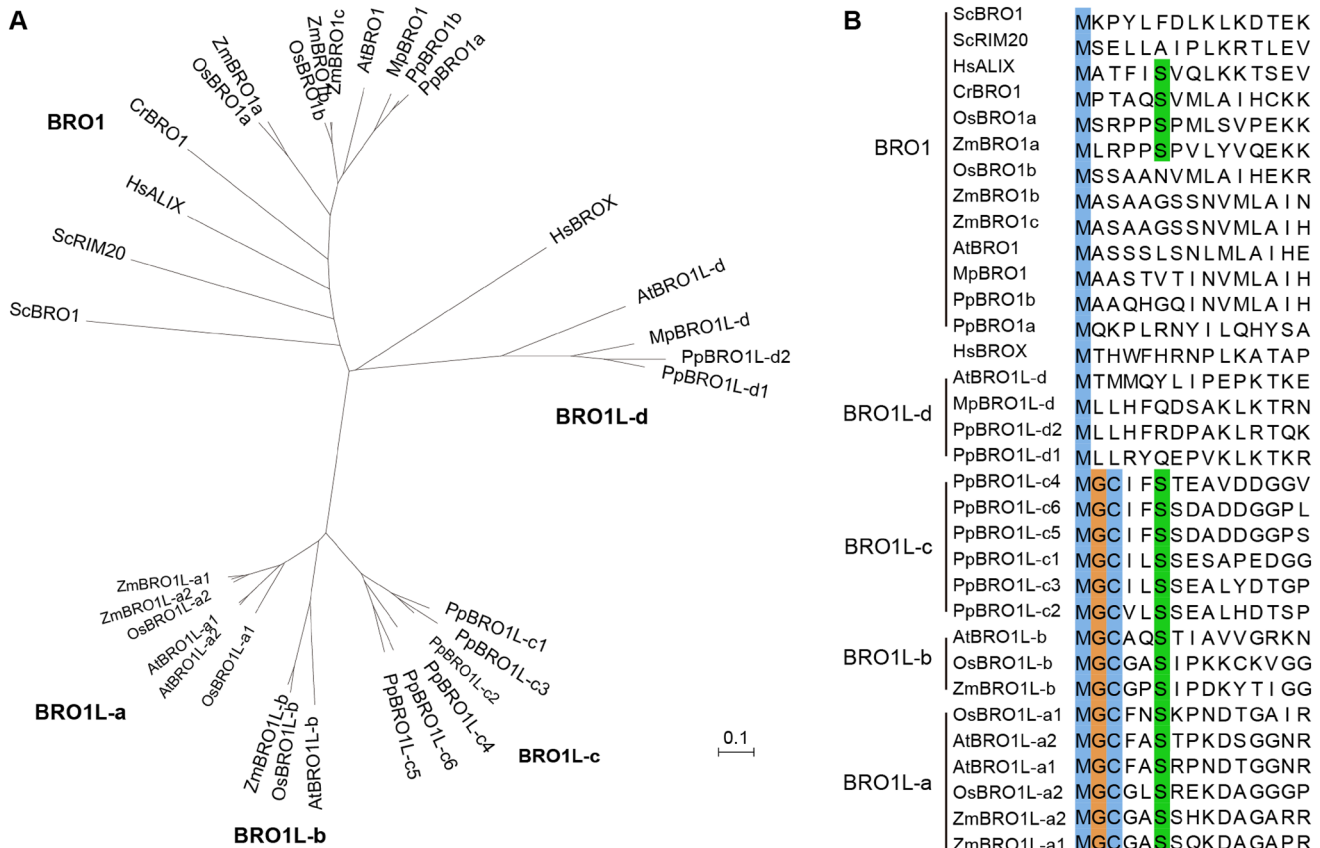


Fig. 4 Phylogenetic tree and N-terminal sequences of BRO1-like proteins. **A** BRO1-like proteins are arranged into four groups. The clade **a-c** are clustered together, while the clade **d** is closely associated with

BRO1. **B** The unaligned N-terminal 15 aa of each protein are shown. Conserved residues potentially involved in MYR are highlighted

(Fig. 5). As the evolutionary origin of the ARF superfamily seems to be complex, it is difficult to conclude how MYR signals may have emerged. Nevertheless, consistent with our findings, MYR features of SARA, ARFs, and ARLs are also similar in other eukaryotes (Vargova et al. 2021): ARFs are mostly MYRed; ARLs display variable levels of MYR; SARA does not undergo MYR. In addition, the evolution of MYR motifs could be coupled to additional domains of ARFs that are required for membrane association (Matheson et al. 2008).

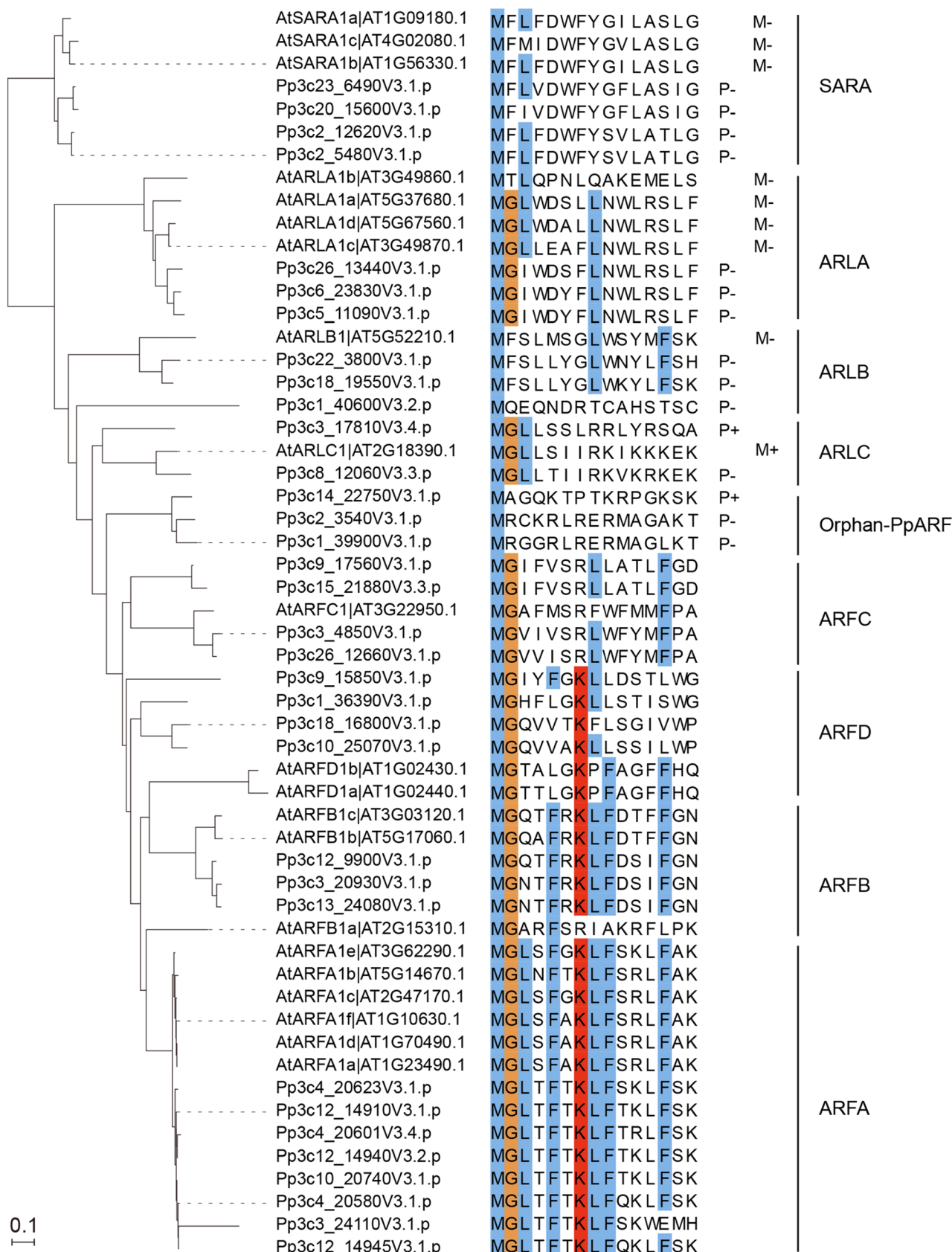
Unlike the ARF superfamily, Rab GTPases employ a C-terminal prenylation signal for membrane anchoring (Shinde and Maddika 2018). Our prediction identified three RABs that undergo MYR of high probability. These proteins lack the prenylation signals and are homologous to the Arabidopsis RABF1/ARA6, which is known to be MYRed in vitro and in vivo (Ueda et al. 2001; Boisson et al. 2003). We asked whether other RABs might be also MYRed. In the Phytozome database, we identified 57 RABs in *P. patens* and they organize into 10 clades, namely RABA1/A2, RABA3/A4, RABA5/A6, RABB, RABC, RABD, RABE, RABF1/F2, RABG, and RABH (Shinde and Maddika 2018)

(Figure S2). Only the RABF1 subgroup contains a classical MGCXXS dual lipidation signal, which is essential for membrane association in Arabidopsis (Ueda et al. 2001). Homology analyses did not reveal Myri-type RABs in algae. Thus, instead of using canonical Cys-containing motifs (usually Cys-Cys or Cys-X-Cys), land plants have uniquely evolved differential lipid modification signals for membrane association of Rab GTPase members.

Calcium-dependent protein kinases

We next analyzed phosphorylation and calcium-related signaling proteins that have been overrepresented in our prediction results. Of these, we selected calcium-dependent protein kinases (CDPKs or CPKs), calcineurin B-like proteins (CBLs), brassinosteroid-signaling kinases (BSKs), and protein phosphatases type 2C (PP2C) because many of them have been shown to undergo MYR and exhibit membrane localization.

In the *P. patens* genome, we identified 27 CDPKs and 5 CDPK-related kinases (CRKs), which is slightly fewer than the Arabidopsis CDPKs and CRKs (34 CDPKs and 8 CRKs)



◀Fig. 5 Phylogenetic tree and N-terminal sequences of Arf GTPases in Arabidopsis and *P. patens*. The moss ARFs are organized into nine groups with an additional moss-specific orphan group compared to the Arabidopsis ARFs. All members of Arabidopsis ARFA-ARFD are MYRed in vitro and their homologs in *P. patens* are predicted to be MYRed by at least one method. MYR status and prediction results of Arabidopsis and moss ARLA-ARLC and SARA proteins are indicated. M+ and M- indicate MYRed and not MYRed in vitro, respectively. P+ and P- indicate positive or negative prediction results, respectively. Note that Ser at position 6 is mostly absent and there is an enrichment of large hydrophobic residues. The unaligned N-terminal 15 aa of each protein are shown. Conserved residues are highlighted

(Nemoto et al. 2015; Shi et al. 2018). Phylogenetic analyses classified the moss CDPK/CRK family into six large groups, CPK-a to CPK-e and CRK, of which CPK-e is a moss-specific clade (Fig. 6). In general, the CRK group has a highly conserved MGXCX(S/G)(K/R) motif at the N-terminus; the CPK-c and CPK-d groups tend to carry an MGNCC or MGXC(S/T) motif; the N-termini of CPK-a and CPK-b groups are more variable, of which some members contain MGNX(C/S) or MGCXSXK ends that favor MYR. Only the CPK-e clade and a few members of CPK-a are strongly against the possibility of MYR. Indeed, all AtCPKs/AtCRKs except four CPK-a proteins are identified in the Arabidopsis myristoylome (Castrec et al. 2018). These data indicate that the N-terminal MYR signal is associated with the functional diversification of CDPKs as early as in the basal land plants.

Protein phosphatases type 2C

The PP2C-related phosphatases are another group of proteins predicted to undergo MYR with high probability. To ask how MYR signals might be associated with PP2C evolution, we identified the entire PP2C family genes in *P. patens*. The Arabidopsis genome encodes 82 PP2C genes (Fuchs et al. 2013). Comparably, we found 93 PP2Cs in *P. patens* and classified them into 15 groups according to (Fuchs et al. 2013), of which the M and N clades were additionally defined (Figure S3). The predicted PP2C genes belong to the A, C, E, I, and L clades. Interestingly, only C, E, I, and L clades were found to preferentially contain an MG N-terminus. The presence of a single MYR target candidate in clade A indicates a de novo introduction in *P. patens*. In general, MYR proteins of the PP2C family have MGXXXS motifs and the clade L and E contain additional Cys residues at position 3 and 4 (Fig. 7). Members of clade I and L are all MYRed in Arabidopsis (Castrec et al. 2018) and predicted to undergo MYR (≥ 1 prediction method) in *P. patens*. By contrast, at least one member of the C and E clades has lost a functional MYR motif. Thus, MYR is limited to only a few PP2C subgroups and displays variability in the clade C and E. This feature is conserved and may have been established in the land plant ancestor.

Calcineurin B-like proteins

We next analyzed CBL proteins. CBLs are plant-type calcium sensors related to the animal Calcineurin phosphatase regulatory subunit Calcineurin B (Tang et al. 2020). Our prediction identified two CBL proteins and one CBL-like EF-hand protein of high MYR probability. CBLs are short and highly similar to Calmodulins, thus making them difficult to be clearly defined (Mohanta et al. 2015). We searched for all CBL and CBL-like genes in *P. patens* and other model plants (liverwort, rice, and maize) to construct preliminary phylogenetic trees with all BLAST-retrieved sequences. This led us to obtain five CBLs in *P. patens* (Kleist et al. 2014; Beckmann et al. 2016), three in *M. polymorpha* (Edel and Kudla 2015), 10 in Arabidopsis (Kolukisaoglu et al. 2004), 10 in *O. sativa* (Kolukisaoglu et al. 2004), and 11 in *Z. mays* (Zhang et al. 2016b), which are mostly consistent with previous reports. However, the predicted CBL-like EF-hand protein (Pp3c15_200) does not fall into the CBL group. This protein contains an FRQ1 superfamily domain as all CBLs do. We carefully filtered out all FQR1 domain-containing proteins outside the CBL clade and found that they form another group here referred to as FRQ1 (Fig. 8). In the CBL clade, MYR signals are clustered specifically in the AtCBL1/4/5/8/9 subgroup and contain an additional Cys3 for palmitoylation (Fig. 8). However, in any of the examined organisms, there is one member that lacks an MYR motif, suggesting that non-MYRed CBL might play important roles in land plants. In mosses, PpCBL2 is also a putative MYR target, while its closely related homologs are not. Thus, PpCBL2 seems to be a species-specific MYR target. In the FRQ1 group, only a few members of each organism have the MGXXXS motif (Fig. 8). Although not common, these motifs are presumably functional because two of them in mosses are predicted to be MYR targets and one Arabidopsis protein could be MYRed in vitro (Castrec et al. 2018). Overall, the data suggest diverse potentialities of MYR in CBLs and related FRQ1 domain-containing proteins for subcellular organization, and this feature is conserved in basal land plants.

Brassinosteroid-signaling kinases

Finally, we investigated brassinosteroid-signaling kinases (BSKs) which receive signals from BR receptors and activate downstream effectors (Tang et al. 2008; Nolan et al. 2020). There are 12 and six members in Arabidopsis and *P. patens*, respectively (Li et al. 2019). Our prediction identified six BSKs of high MYR probability, including two that have not been reported (Table S2). Domain analyses revealed that they lack the tetratricopeptide repeats (TPRs) at the C-termini. TPRs can directly bind the N-terminal kinase domain and inhibit OsBSK3 activity in rice (Zhang et al.

Fig. 6 Phylogenetic tree and N-terminal sequences of CDPKs/CRKs in *Arabidopsis* and *P. patens*. The moss CDPKs are organized into five groups (CPK-a to CPK-e) with the CPK-e clade being moss-specific. The CRKs contain a conserved MGXCX(S/G) (R/K) motif. CDPKs have more variable N-termini and several members of CPK-a are not favored for MYR. The PpCPK-e2 sequence is incomplete in the Phytozome database. The unaligned N-terminal 15 aa of each protein are shown. M+ and M- indicate MYRed and not MYRed in vitro, respectively. P+ and P- indicate positive or negative prediction results, respectively. Conserved residues within each group are highlighted

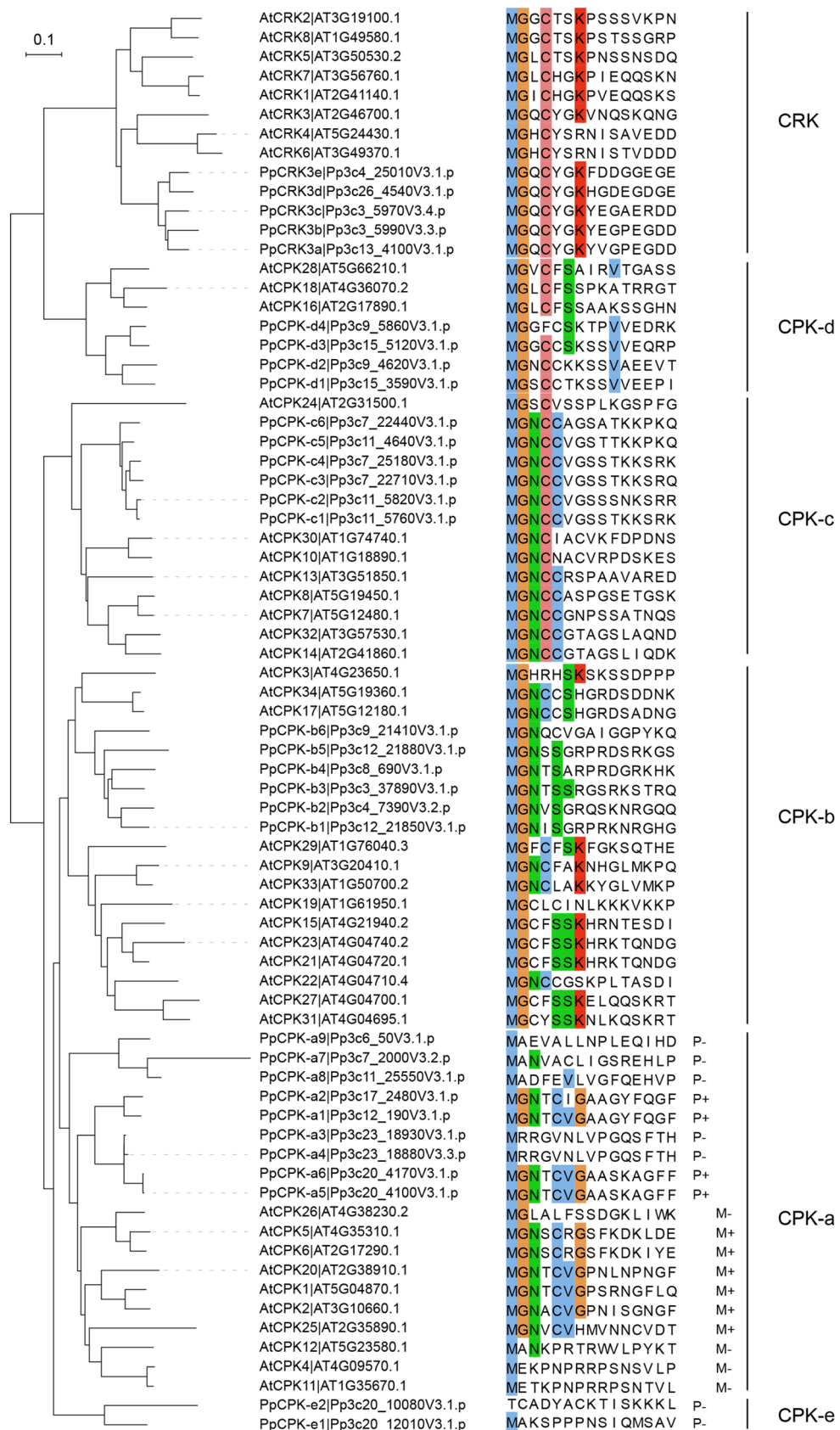
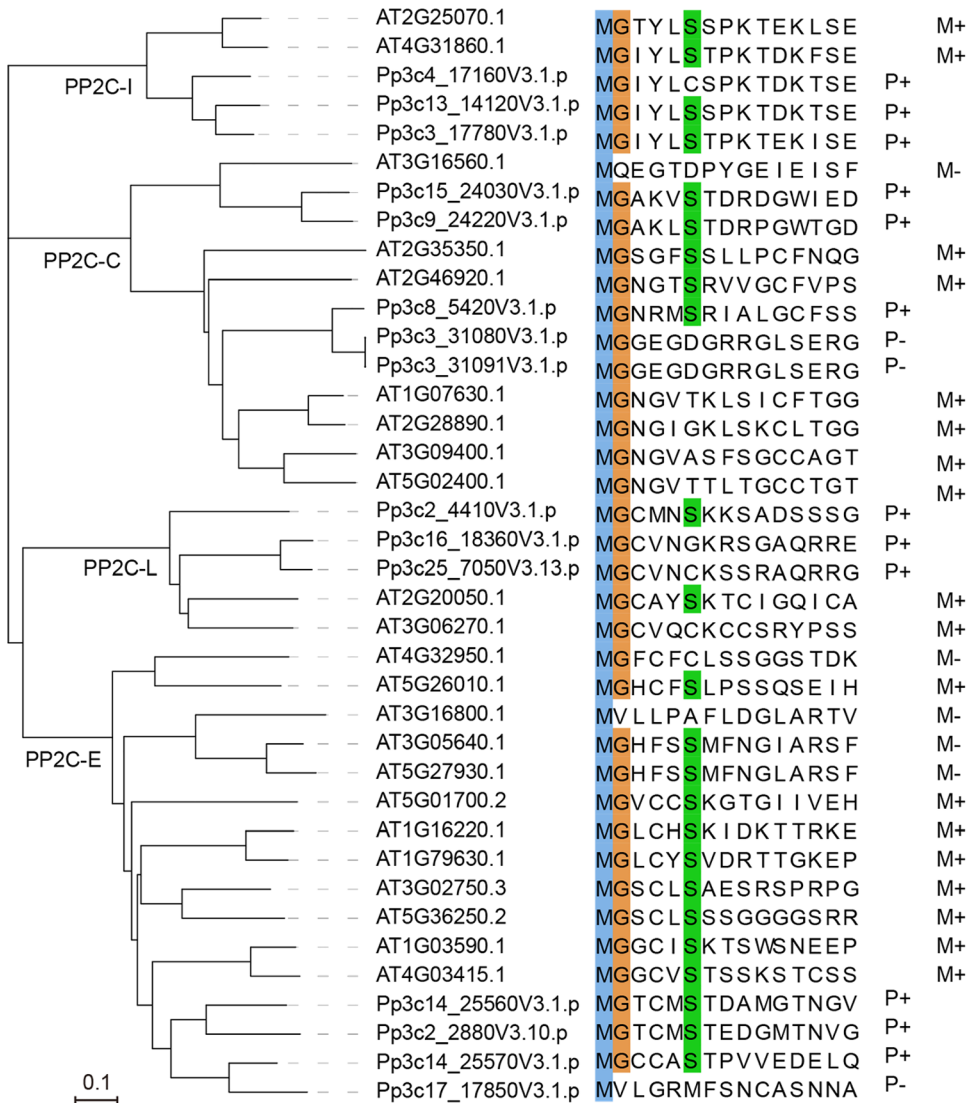


Fig. 7 Phylogenetic tree and N-terminal sequences of PP2C-I/C/L/E clades in *Arabidopsis* and *P. patens*. The majority of PP2C-I/C/L/E clade members have an MGXXXS motif. Clade L and E also preferentially contain Cys at position 3 and 4. The unaligned N-terminal 15 aa of each protein are shown. M+ and M- indicate MYRed and not MYRed in vitro, respectively. P+ and P- indicate positive or negative prediction results, respectively. Conserved residues are highlighted



2016a). However, TPRs are not essential for BSK function (Zhang et al. 2016a; Ren et al. 2019). Thus, we designated these two genes as BSKs. BSKs have originated in land plants (Wang et al. 2015) and form a unique clade in bryophytes (Fig. 9A). The eight PpBSKs exist in two subgroups and are designated PpBSK-a and PpBSK-b. Alignment of BSK sequences from major model plants shows a common MGXXXS motif and a Cys at position 3–5 in the majority of BSKs, indicative of dual lipid modification. Indeed, most of the BSKs in *Arabidopsis* are MYRed in vitro (Castrec et al. 2018) and have been reported to localize at the PM (Tang et al. 2008; Bayer et al. 2009; Shi et al. 2013; Sreeramulu et al. 2013; Majhi et al. 2019, 2021; Ren et al. 2019; Su et al. 2021, 2022). In *P. patens*, rice, and maize, there is one BSK that lacks an MYR signal. They might play distinct functions in an organism-specific manner. For example, the moss PpBSK-a1 has an acidic residue (Glu113) instead of a critical Lys corresponding to AtBSK1^{104K} for ATP-binding;

the rice OsBSK3 lacks a significant portion of the kinase domain based on the updated gene model in Phytozome which is different from (Zhang et al. 2016a); both PpBSK-a1 and ZmBSK7 have extended or shortened segments in the kinase domain. Nevertheless, MYR signals have been largely retained since the introduction of BSKs into land plants (Wang et al. 2015) and should be important for their membrane localization.

To test whether an MYR motif in *P. patens* BSKs could enable membrane targeting, we generated a transgenic mCherry reporter (Myri-mCherry) fused with the N-terminal peptide (MGCFSSKPK) of PpBSK-b4. As expected, the mCherry signal was exclusively detected on the PM (Fig. 9B). Additionally, we observed a slight enrichment at the tip of growing cells. Myri-mCherry signals could quantitatively reflect membrane amount as the cross membrane at cell–cell contacting sites displayed a ~ twofold higher intensity than the lateral membrane (two versus one membrane)

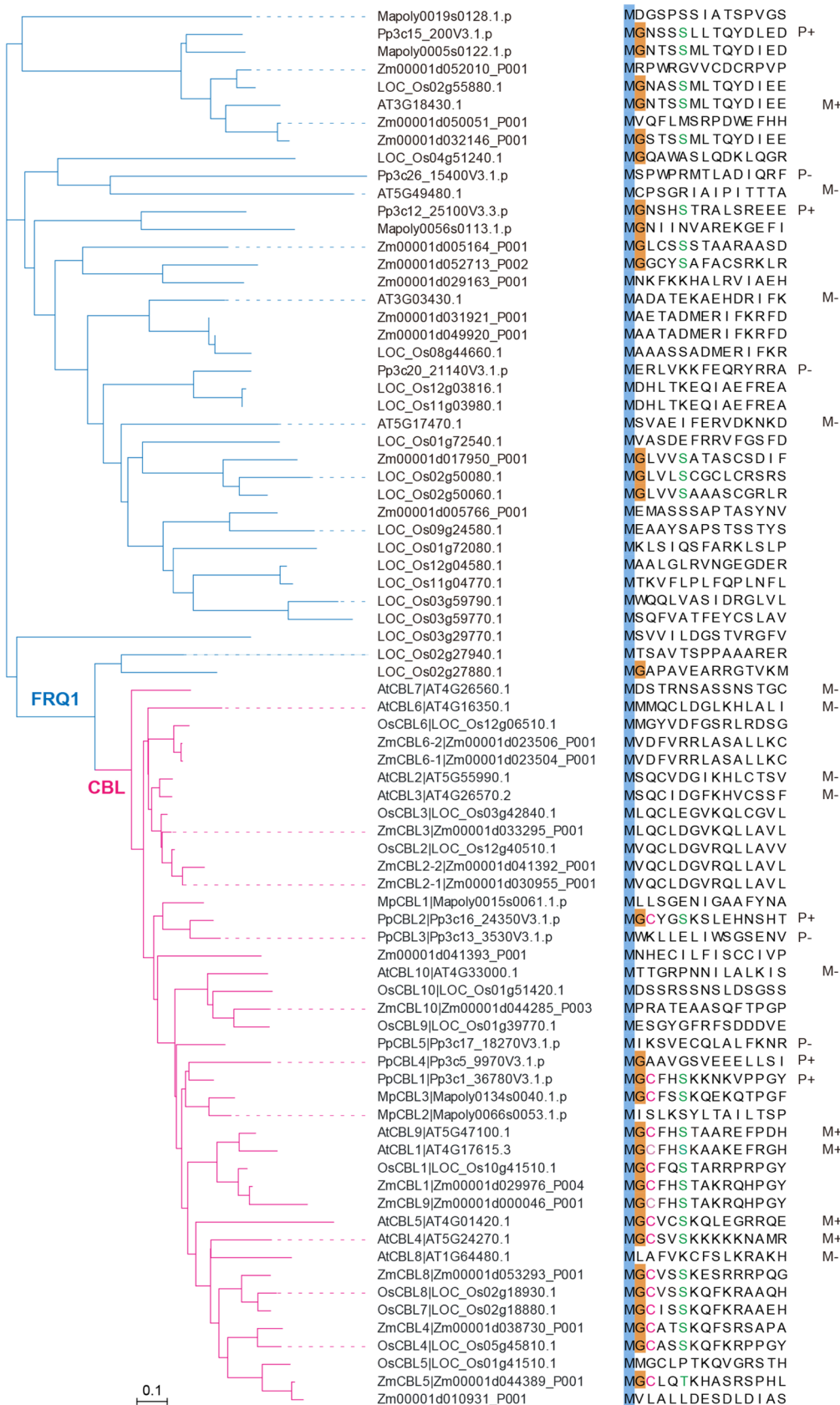


Fig. 8 Phylogenetic tree and N-terminal sequences of CBLs and FRQ1 domain-containing proteins. FRQ1 and CBL proteins are identified with an FRQ1 domain. The unaligned N-terminal 15 aa of each protein are shown. M+ and M− indicate MYRed and not MYRed in vitro, respectively. P+ and P− indicate positive or negative prediction results, respectively. The MGXXXS or MGCXX(S/T) motifs are indicated

(Fig. 9B and C). In tip-growing cells, a gradual decrease of mCherry signals was observed from the tip to the basal region (Fig. 9D), suggesting that membrane lipids are more concentrated at the growth region. To further test this, we examined the localization ROP4 which polarizes tip cells for growth (Yi and Goshima 2020). As expected, both Myr-mCherry and ROP4 were accumulated on the apical membrane with ROP4 localizing at a more distal region (Fig. 9E). We next performed time-lapse imaging at the expanding and mature (non-expanding) regions and observed a decrease of intensity in the expanding but not mature membranes (Fig. 9F and G, Movie S1). These data collectively indicate that lipid distribution is correlated with cell growth, which is consistent with quantitative results from pollen tubes (Grebnev et al. 2020) and the model of vesicle delivery and membrane expansion in tip-growing cells (Guo and Yang 2020).

Discussion

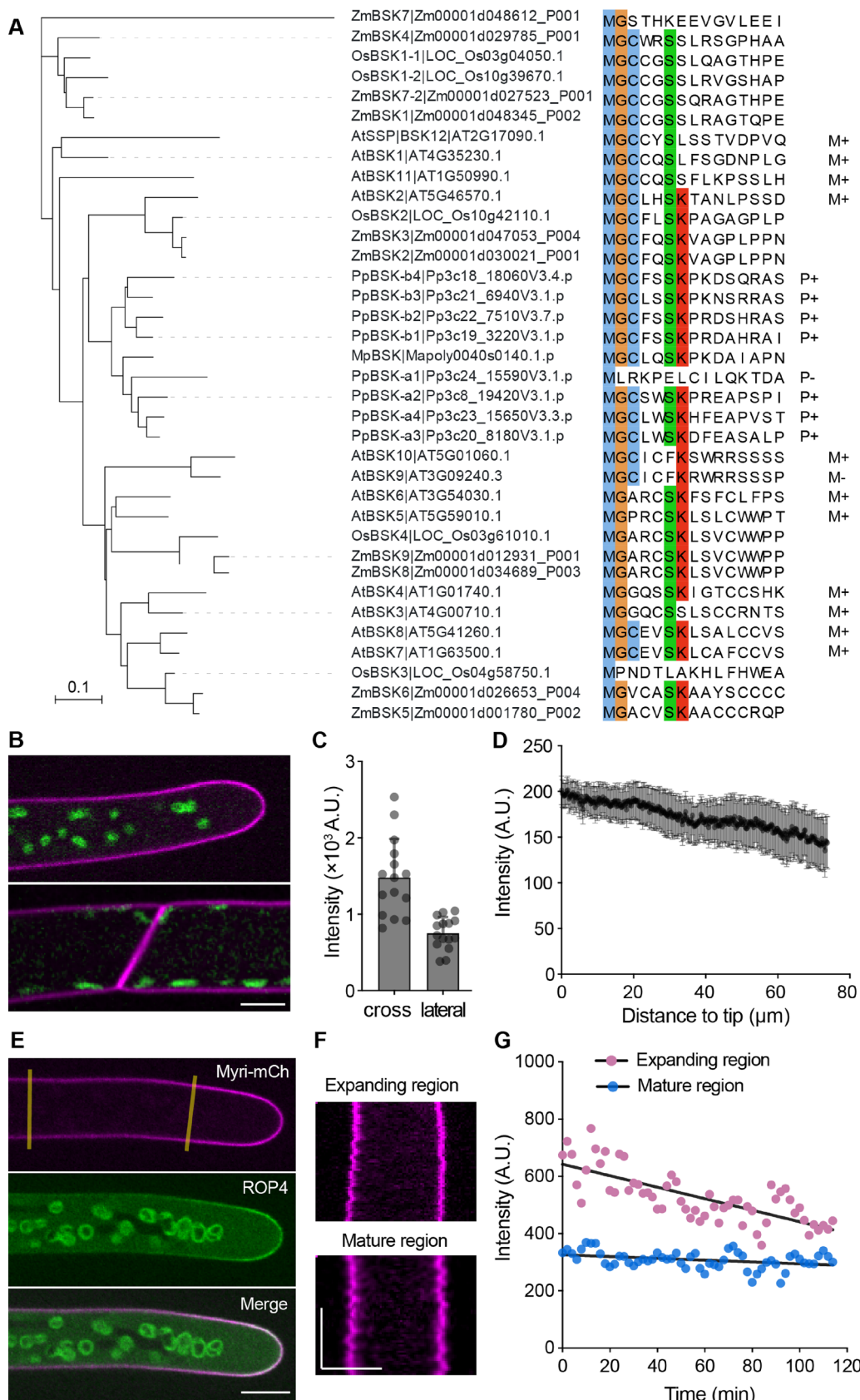
In this study, we report the characterization of the putative myristoylome of the moss *P. patens*. Our data provide a valuable resource for future studies on MYR and its functional relevance in basal land plants. Although experimental studies are needed to verify the putative MYR targets, our results provide evidence that it is possible to identify true targets via multiple prediction tools because many of our top hits have homologs that are MYRed in vitro and in vivo. This is consistent with presumably similar enzymatic activities and substrate recognition mechanisms by NMTs in land plants and animals (Fig. 1B). Additionally, our results indicate that prediction could potentially identify novel targets because 16% of our top hits are moss or bryophyte-specific.

The membrane-targeting ability of MYR signals is conserved in basal land plants. MYRed proteins, such as BRO1L (Shen et al. 2018), ARF GTPases (Matheson et al. 2008), CBLs (Ishitani et al. 2000; Xu et al. 2006; Cheong et al. 2007; Batistic et al. 2008; Zhang et al. 2016b; Saito et al. 2018), CDPKs (Rutschmann et al. 2002; Dammann et al. 2003; Mehlmer et al. 2010; Zou et al. 2010; Gutermuth et al. 2013; Lu and Hrabak 2013; Saito et al. 2018; Khalid et al. 2019), PP2C (Gagne and Clark 2010; Tsugama et al. 2012b, 2012a), and BSKs (Tang et al. 2008; Shi et al. 2013; Sreeramulu et al. 2013; Majhi et al. 2019, 2021; Ren et al. 2019; Su et al. 2022) in flowering plants, have been reported to primarily localize at the plasma

membrane. There have been few reports on MYR-mediated targeting in basal land plants. Our study shows that the MYR motif of PpBSK-b4 is capable of membrane targeting. This motif is highly conserved in various species, including moss, liverwort, Arabidopsis, rice, and maize. Therefore, we conclude that MYR-mediated membrane targeting is an ancient mechanism used for protein localization in land plants.

How do MYR signals change during evolution? In all analyzed MYR substrate candidates, MYR target motif-containing proteins are clustered in specific groups, indicating a high correlation between MYR signal and protein function during evolution. However, some members of the same protein family such as CBLs have gained or lost MYR target motifs (Fig. 8). Therefore, MYR signals can be dynamically introduced or lost to presumably mediate alternative protein distribution. This not only occurs in a protein group of the same organism but is also found at the organismal level. For example, the VID27 domain-containing protein is conserved in eukaryotes and has evolved an MYR signal in green algae (Figure S4). However, the MYR motif seems to be lost specifically in *Selaginella moellendorffii*. These results revealed the dynamic nature of MYR signal evolution which may be important for the specialized compartmentalization of certain proteins in an organism-specific manner. For instance, the R-SNARE VAMP72 proteins in *M. polymorpha* have been reported to contain a unique MYR signal for membrane targeting (Kanazawa et al. 2016).

In addition to membrane-associated components, our prediction also revealed the enrichment of nuclear-localized proteins (Fig. 3B). Nuclear proteins have been considered false-positive hits by MYR prediction (Podell and Gribskov 2004). However, MYR may play unconventional roles outside the PM and membrane organelles. For example, the 26S proteasome regulatory subunit RPT2 is MYRed in yeasts (Kimura et al. 2003) and Arabidopsis (Boisson et al. 2003), but the yeast RPT2 is mainly localized in the nucleus and this localization requires the MYR signal (Kimura et al. 2012). Arabidopsis homologs of several predicted MYR substrates are MYRed in vitro (Castrec et al. 2018) and have been reported to display nuclear localization such as LUL3/VBP1 (Chung et al. 2013), UBP4 (Chandler et al. 1997), and PSI2 (Stuhrwohldt et al. 2014). In addition, the DUF630 and DUF632 domain-containing putative DNA ligase, which is specifically present in land plants, has a highly conserved MGCXXS motif in most members, suggesting a strong probability of MYR and S-acylation (Figure S5). Nevertheless, future studies are required to illustrate the physiological function of putative MYR signals. At least in some reports, such as (Stuhrwohldt et al. 2014), the MYR signal is neither required for membrane localization nor protein function, even though MYR has been observed in vitro (Castrec et al. 2018). It is tempting to speculate that MYR might mediate



◀Fig. 9 Phylogenetic analyses of BSKs and membrane targeting by the MYR signal of PpBSK-b4. **A** Phylogenetic tree and N-terminal sequences of BSKs. The majority of BSK members have an MGXXXX motif and contain an additional Cys residue at position 3–5 and a Lys at position 7. The unaligned N-terminal 15 aa of each protein are shown. M+ and M− indicate MYRed and not MYRed in vitro, respectively. P+ and P− indicate positive or negative prediction results, respectively. Conserved residues are highlighted. **B** Membrane localization of mCherry fused with the MYR signal (MGCFSSKPK) of PpBSK-b4. Magenta, mCherry signal; Green, chloroplasts (**C**) Quantification of Myri-mCherry fluorescence intensity at the cross or lateral membranes ($n=15$, mean \pm SD). **D** Fluorescence intensity in tip-growing cells ($n=16$, mean \pm SEM). **E** Colocalization of Myri-mCherry (magenta) and mNG-ROP4 (green). Yellow lines indicate the expanding and mature (non-expanding) regions. **F** Representative kymographs of membranes at selected regions in (**E**). **(G)** Intensity plot over time for signals shown in (**F**). Scale bars: horizontal, 10 μ m (**B**, **E**, and **F**); vertical, 1 h (**F**)

protein relocation under specific conditions such as biotic and abiotic stresses.

Materials and methods

Prediction of MYR targets in *Arabidopsis* and *P. patens*

Proteins sequences of *Arabidopsis* (version: Araport11) and the moss *P. patens* (version: v3.3) were obtained from the Phytozome database (<https://phytozome-next.jgi.doe.gov>). Generally, each gene was represented by the longest isoform. If the Met-Gly terminus was not present in the longest isoform but existed in a shorter isoform, the shorter Met-Gly-starting isoform was used. The first 30 amino acids of Met-Gly-starting proteins were extracted and subject to prediction with the following tools: NMT predictor (Maurer-Stroh et al. 2002), PlantsP (Podell and Gribkoff 2004), Expasy myristoylator (Bologna et al. 2004), SVMYr (Madeo et al. 2022), Terminator3 (Martinez et al. 2008), and GPS-lipid (Xie et al. 2016). The presumably complete *Arabidopsis* myristoylome (Castrec et al. 2018) was used for the comparison and identification of moss homologs. Briefly, *Arabidopsis* gene IDs were mapped in Phytozome. Moss homologs were identified either by homolog retrieval with PhytoMine or BLASTing *Arabidopsis* sequences against the *P. patens* proteome with a filter of E-value below 10^{-50} . The identified homologs were pooled with prediction hits by NMT predictor, PlantsP, Expasy, and SVMYr, yielding the putative myristoylome of *P. patens*.

Sequence alignment and phylogenetic tree construction

Homologous proteins in selected organisms were identified by BLASTing against the reference genomes in

Phytozome or Uniprot (<http://www.uniprot.org>) and were manually inspected. Sequences of *Porphyra umbilicalis*, *Chlamydomonas reinhardtii*, *Physcomitrium patens*, *Marchantia polymorpha*, *Selaginella moellendorffii*, *Arabidopsis thaliana*, *Oryza sativa subsp. japonica* and *Zea mays* were retrieved from Phytozome. Sequences of *Saccharomyces cerevisiae*, *Chara braunii*, *Caenorhabditis elegans*, *Drosophila melanogaster*, *Danio rerio*, *Mus musculus*, and *Homo sapiens* were obtained from UniProt. Alignment was performed using the online MAFFT service incorporated in Jalview (<https://www.jalview.org>). Phylogenetic trees were constructed in MEGA11 (<https://www.megasoftware.net>) using the neighbor-joining method with default parameters. Trees were rendered with the iTOL online tool (<https://itol.embl.de>). Domain search was performed in the NCBI CDD database (<https://www.ncbi.nlm.nih.gov/Structure/cdd/wrpsb.cgi>).

Gene ontology analyses

Gene ontology (GO) analyses were performed with the Blast2GO module from OmicsBox. Briefly, full-length sequences of predicted MYR targets were input for BLAST against the NCBI proteome database. GO terms for mapped sequences were retrieved by EMBL-EBI InterProScan or by a search for associated GO terms in the NCBI database. Sequences were additionally annotated by the EggNOG mapper. All returned results were merged and cleared for duplications. The annotation summary of the entire set of proteins was generated by the Combined Graph tool. Enrichment analyses were performed with Fisher's Exact Test (two-tailed, $p=0.025$ non-adjusted) to compare hits predicted by ≥ 3 and < 3 methods in the putative moss myristoylome.

Moss culture and transgenesis

Moss cultivation, transformation, and imaging procedures in this study followed (Yamada et al. 2016) with minor modifications. In brief, mosses were cultured on BCDAT solid medium under continuous light. The N-terminal sequence of PpBSK-b4 (Pp3c18_18060) encoding the first nine amino acids was cloned into the pTM412 (pENTR-mCherry) vector at the N-terminus of mCherry. The resultant Myri-mCherry sequence was inserted into pMN601 via LR reaction using the Gateway LR Clonase II Enzyme Mix (Invitrogen, cat. 11,791–020), generating the overexpression plasmid. Myri-mCherry was expressed under the control of EF1 α promoter. The expression cassette together with a Nourseothricin-resistance selection marker was transformed into wild-type mosses. Stably integrated transgenic lines were used for confocal microscopy imaging.

Imaging and data analyses

Moss protonema tissues were inoculated on BCD solid medium in 35-mm bottom-glass dishes. After 5~7 days' culture, cells were imaged using a Nikon Ti microscope equipped with a CSU-X1 spinning disk confocal scanner unit (Yokogawa), an EMCCD camera (ImagEM, Hamamatsu), a $60 \times 1.40\text{-NA}$ or $40 \times 1.30\text{-NA}$ lens, and 561 nm and 488 nm laser lines (LDSYS-488/561-50-YHQSP3, Pneum). Time-lapse imaging was performed at an interval of 2 min. Fluorescence intensity at the cross and lateral membranes for quantification was measured at line-selected regions of the same size. In tip cells, intensity measurement was performed for a ~70 μm -long region along the growth direction starting from a point 4 μm distant to the very tip. All values were subtracted by a background measurement.

Supplementary Information The online version contains supplementary material available at <https://doi.org/10.1007/s00299-023-03016-7>.

Acknowledgements We thank Prof. Gohta Goshima for providing the pTM412 and pMN601 plasmids.

Author contribution statement PY and CX: conceptualized this project. LL, JR, and PY: performed the experiments and analyzed the data. PY and CX: wrote the manuscript.

Funding This study was funded by National Natural Science Foundation of China (32100273, 32270776), Sichuan University (1082204112609, 2022SCUH0010), and People's Government of Sichuan Province.

Data availability All relevant data are available within the manuscript and the supporting materials.

Declarations

Conflict of interest The authors declare no conflict of interest.

References

- Ashrafi K, Farazi TA, Gordon JI (1998) A role for *Saccharomyces cerevisiae* fatty acid activation protein 4 in regulating protein N-myristoylation during entry into stationary phase. *J Biol Chem* 273:25864–25874
- Batistic O, Sorek N, Schultke S, Yalovsky S, Kudla J (2008) Dual fatty acyl modification determines the localization and plasma membrane targeting of CBL/CIPK Ca²⁺ signaling complexes in *Arabidopsis*. *Plant Cell* 20:1346–1362
- Bayer M, Nawy T, Giglione C, Galli M, Meinnel T, Lukowitz W (2009) Paternal control of embryonic patterning in *Arabidopsis thaliana*. *Science* 323:1485–1488
- Beckmann L, Edel KH, Batistic O, Kudla J (2016) A calcium sensor - protein kinase signaling module diversified in plants and is retained in all lineages of Bikonta species. *Sci Rep* 6:31645
- Bhatnagar RS, Futterer K, Farazi TA, Korolev S, Murray CL, Jackson-Machelski E, Gokel GW, Gordon JI, Waksman G (1998) Structure of N-myristoyltransferase with bound myristoylCoA and peptide substrate analogs. *Nat Struct Biol* 5:1091–1097
- Boisson B, Giglione C, Meinnel T (2003) Unexpected protein families including cell defense components feature in the N-myristoylome of a higher eukaryote. *J Biol Chem* 278:43418–43429
- Bologna G, Yvon C, Duvaud S, Veuthey AL (2004) N-Terminal myristylation predictions by ensembles of neural networks. *Proteomics* 4:1626–1632
- Castrec B, Dian C, Ciccone S, Ebert CL, Bienvenut WV, Le Caer JP, Steyaert JM, Giglione C, Meinnel T (2018) Structural and genomic decoding of human and plant myristoylomes reveals a definitive recognition pattern. *Nat Chem Biol* 14:671–679
- Chandler JS, McArdele B, Callis J (1997) AtUBP3 and AtUBP4 are two closely related *Arabidopsis thaliana* ubiquitin-specific proteases present in the nucleus. *Mol Gen Genet* 255:302–310
- Cheong YH, Pandey GK, Grant JJ, Batistic O, Li L, Kim BG, Lee SC, Kudla J, Luan S (2007) Two calcineurin B-like calcium sensors, interacting with protein kinase CIPK23, regulate leaf transpiration and root potassium uptake in *Arabidopsis*. *Plant J* 52:223–239
- Chung E, Cho CW, So HA, Kang JS, Chung YS, Lee JH (2013) Over-expression of VrUBC1, a Mung Bean E2 Ubiquitin-conjugating enzyme, enhances osmotic stress Tolerance in *Arabidopsis*. *PLoS ONE* 8:e66056
- Dammann C, Ichida A, Hong B, Romanowsky SM, Hrabak EM, Harmon AC, Pickard BG, Harper JF (2003) Subcellular targeting of nine calcium-dependent protein kinase isoforms from *Arabidopsis*. *Plant Physiol* 132:1840–1848
- Dian C, Perez-Dorado I, Riviere F, Asensio T, Legrand P, Ritzefeld M, Shen M, Cota E, Meinnel T, Tate EW, Giglione C (2020) High-resolution snapshots of human N-myristoyltransferase in action illuminate a mechanism promoting N-terminal Lys and Gly myristoylation. *Nat Commun* 11:1132
- Duronio RJ, Reed SI, Gordon JI (1992) Mutations of human myristoyl-CoA:protein N-myristoyltransferase cause temperature-sensitive myristic acid auxotrophy in *Saccharomyces cerevisiae*. *Proc Natl Acad Sci U S A* 89:4129–4133
- Edel KH, Kudla J (2015) Increasing complexity and versatility: how the calcium signaling toolkit was shaped during plant land colonization. *Cell Calcium* 57:231–246
- Fuchs S, Grill E, Meskiene I, Schweighofer A (2013) Type 2C protein phosphatases in plants. *FEBS J* 280:681–693
- Gagne JM, Clark SE (2010) The *Arabidopsis* stem cell factor POLTERGEIST is membrane localized and phospholipid stimulated. *Plant Cell* 22:729–743
- Giglione C, Meinnel T (2021) Mapping the myristoylome through a complete understanding of protein myristylation biochemistry. *Prog Lip Res* 85:101139
- Glover CJ, Hartman KD, Felsted RL (1997) Human N-myristoyltransferase amino-terminal domain involved in targeting the enzyme to the ribosomal subcellular fraction. *J Biol Chem* 272:28680–28689
- Grebnev G, Cvitkovic M, Fritz C, Cai G, Smith AS, Kost B (2020) Quantitative structural organization of bulk apical membrane traffic in pollen tubes. *Plant Physiol* 183:1559–1585
- Guo J, Yang Z (2020) Exocytosis and endocytosis: coordinating and fine-tuning the polar tip growth domain in pollen tubes. *J Exp Bot* 71:2428–2438
- Gutermuth T, Lassig R, Portes MT, Maierhofer T, Romeis T, Borst JW, Hedrich R, Feijo JA, Konrad KR (2013) Pollen tube growth regulation by free anions depends on the interaction between the anion channel SLAH3 and calcium-dependent protein kinases CPK2 and CPK20. *Plant Cell* 25:4525–4543
- Ishitani M, Liu J, Halfter U, Kim CS, Shi W, Zhu JK (2000) SOS3 function in plant salt tolerance requires N-myristylation and calcium binding. *Plant Cell* 12:1667–1678
- Jumper J, Evans R, Pritzel A, Green T, Figurnov M, Ronneberger O, Tunyasuvunakool K, Bates R, Zidek A, Potapenko A, Bridgland A, Meyer C, Kohl SAA, Ballard AJ, Cowie A, Romera-Paredes

- B, Nikolov S, Jain R, Adler J, Back T, Petersen S, Reiman D, Clancy E, Zielinski M, Steinegger M, Pacholska M, Berghammer T, Bodenstein S, Silver D, Vinyals O, Senior AW, Kavukcuoglu K, Kohli P, Hassabis D (2021) Highly accurate protein structure prediction with AlphaFold. *Nature* 596:583–589
- Kanazawa T, Era A, Minamino N, Shikano Y, Fujimoto M, Uemura T, Nishihama R, Yamato KT, Ishizaki K, Nishiyama T, Kohchi T, Nakano A, Ueda T (2016) SNARE molecules in *marchantia polymorpha*: unique and conserved features of the membrane fusion machinery. *Plant Cell Physiol* 57:307–324
- Khalid MHB, Raza MA, Yu HQ, Khan I, Sun FA, Feng LY, Qu JT, Fu FL, Li WC (2019) Expression, subcellular localization, and interactions of CPK family genes in maize. *Int J Mol Sci* 20(24):6173
- Kimura A, Kato Y, Hirano H (2012) N-myristoylation of the Rpt2 subunit regulates intracellular localization of the yeast 26S proteasome. *Biochemistry* 51:8856–8866
- Kimura Y, Saeki Y, Yokosawa H, Polevoda B, Sherman F, Hirano H (2003) N-Terminal modifications of the 19S regulatory particle subunits of the yeast proteasome. *Arch Biochem Biophys* 409:341–348
- Kleist TJ, Spencley AL, Luan S (2014) Comparative phylogenomics of the CBL-CIPK calcium-decoding network in the moss *Physcomitrella*, *Arabidopsis*, and other green lineages. *Front Plant Sci* 5:187
- Kolukisaoglu U, Weinl S, Blazevic D, Batistic O, Kudla J (2004) Calcium sensors and their interacting protein kinases: genomics of the *Arabidopsis* and rice CBL-CIPK signaling networks. *Plant Physiol* 134:43–58
- Kosciuk T, Price IR, Zhang X, Zhu C, Johnson KN, Zhang S, Halaby SL, Komaniecki GP, Yang M, DeHart CJ, Thomas PM, Kelleher NL, Fromme JC, Lin H (2020) NMT1 and NMT2 are lysine myristoyltransferases regulating the ARF6 GTPase cycle. *Nat Commun* 11:1067
- Li Z, Shen J, Liang J (2019) Genome-wide identification, expression profile, and alternative splicing analysis of the brassinosteroid-signaling kinase (BSK) family genes in *Arabidopsis*. *Int J Mol Sci* 20:1138
- Lu SX, Hrabak EM (2013) The myristoylated amino-terminus of an *Arabidopsis* calcium-dependent protein kinase mediates plasma membrane localization. *Plant Mol Biol* 82:267–278
- Madeo G, Savojardo C, Martelli PL, Casadio R (2022) SVMYr: a web server detecting co- and post-translational myristylation in proteins. *J Mol Biol* 434:167605
- Majeran W, Le Caer JP, Ponnala L, Meinnel T, Giglione C (2018) Targeted profiling of *arabidopsis thaliana* subproteomes illuminates co- and posttranslationally N-terminal myristoylated proteins. *Plant Cell* 30:543–562
- Majhi BB, Sreramulu S, Sessa G (2019) BRASSINOSTEROID-SIGNALING KINASE5 associates with immune receptors and is required for immune responses. *Plant Physiol* 180:1166–1184
- Majhi BB, Sobol G, Gachie S, Sreramulu S, Sessa G (2021) BRASSINOSTEROID-SIGNALLING KINASES 7 and 8 associate with the FLS2 immune receptor and are required for flg22-induced PTI responses. *Mol Plant Pathol* 22:786–799
- Martinez A, Traverso JA, Valot B, Ferro M, Espagne C, Ephritikhine G, Zivy M, Giglione C, Meinnel T (2008) Extent of N-terminal modifications in cytosolic proteins from eukaryotes. *Proteomics* 8:2809–2831
- Matheson LA, Suri SS, Hanton SL, Chatre L, Brandizzi F (2008) Correct targeting of plant ARF GTPases relies on distinct protein domains. *Traffic* 9:103–120
- Maurer-Stroh S, Eisenhaber B, Eisenhaber F (2002) N-terminal N-myristoylation of proteins: prediction of substrate proteins from amino acid sequence. *J Mol Biol* 317:541–557
- Mehlmer N, Wurzinger B, Stael S, Hofmann-Rodrigues D, Csaszar E, Pfister B, Bayer R, Teige M (2010) The $\text{Ca}^{(2+)}$ -dependent protein kinase CPK3 is required for MAPK-independent salt-stress acclimation in *Arabidopsis*. *Plant J* 63:484–498
- Meinnel T, Dian C, Giglione C (2020) Myristylation, an ancient protein modification mirroring eukaryogenesis and evolution. *Trends Biochem Sci* 45:619–632
- Mohanta TK, Mohanta N, Mohanta YK, Parida P, Bae H (2015) Genome-wide identification of Calcineurin B-Like (CBL) gene family of plants reveals novel conserved motifs and evolutionary aspects in calcium signaling events. *BMC Plant Biol* 15:189
- Nemoto K, Takemori N, Seki M, Shinozaki K, Sawasaki T (2015) Members of the plant CRK superfamily are capable of trans- and autophosphorylation of tyrosine residues. *J Biol Chem* 290:16665–16677
- Nielsen E (2020) The small GTPase superfamily in plants: a conserved regulatory module with novel functions. *Annu Rev Plant Biol* 71:247–272
- Nolan TM, Vukasinovic N, Liu D, Russinova E, Yin Y (2020) Brassinosteroids: multidimensional regulators of plant growth, development, and stress responses. *Plant Cell* 32:295–318
- Odorizzi G, Katzmann DJ, Babst M, Audhya A, Emr SD (2003) Bro1 is an endosome-associated protein that functions in the MVB pathway in *Saccharomyces cerevisiae*. *J Cell Sci* 116:1893–1903
- Pierre M, Traverso JA, Boisson B, Domenichini S, Bouchez D, Giglione C, Meinnel T (2007) N-myristoylation regulates the SnRK1 pathway in *Arabidopsis*. *Plant Cell* 19:2804–2821
- Podell S, Grabskov M (2004) Predicting N-terminal myristylation sites in plant proteins. *BMC Genomics* 5:37
- Qi Q, Rajala RV, Anderson W, Jiang C, Rozwadowski K, Selvaraj G, Sharma R, Datla R (2000) Molecular cloning, genomic organization, and biochemical characterization of myristoyl-CoA:protein N-myristoyltransferase from *Arabidopsis thaliana*. *J Biol Chem* 275:9673–9683
- Ramazi S, Zahiri J (2021) Posttranslational modifications in proteins: resources, tools and prediction methods. *Database (oxford)* 2021:baab012
- Ren H, Willige BC, Jaillais Y, Geng S, Park MY, Gray WM, Chory J (2019) BRASSINOSTEROID-SIGNALING KINASE 3, a plasma membrane-associated scaffold protein involved in early brassinosteroid signaling. *PLoS Genet* 15:e1007904
- Rensing SA, Lang D, Zimmer AD, Terry A, Salamov A, Shapiro H, Nishiyama T, Perroud PF, Lindquist EA, Kamisugi Y, Tanahashi T, Sakakibara K, Fujita T, Oishi K, Shin IT, Kuroki Y, Toyoda A, Suzuki Y, Hashimoto S, Yamaguchi K, Sugano S, Kohara Y, Fujiyama A, Anterola A, Aoki S, Ashton N, Barbazuk WB, Barker E, Bennetzen JL, Blankenship R, Cho SH, Dutcher SK, Estelle M, Fawcett JA, Gundlach H, Hanada K, Heyl A, Hicks KA, Hughes J, Lohr M, Mayer K, Melkozernov A, Murata T, Nelson DR, Pils B, Prigge M, Reiss B, Renner T, Rombauts S, Rushton PJ, Sandersfoot A, Schween G, Shiu SH, Stueber K, Theodoulou FL, Tu H, Van de Peer Y, Verrier PJ, Waters E, Wood A, Yang L, Cove D, Cuming AC, Hasebe M, Lucas S, Mishler BD, Reski R, Grigoriev IV, Quatrano RS, Boore JL (2008) The *Physcomitrella* genome reveals evolutionary insights into the conquest of land by plants. *Science* 319:64–69
- Rutschmann F, Stalder U, Piotrowski M, Oecking C, Schaller A (2002) LeCPK1, a calcium-dependent protein kinase from tomato. Plasma membrane targeting and biochemical characterization. *Plant Physiol* 129:156–168
- Saito S, Hamamoto S, Moriya K, Matsuura A, Sato Y, Muto J, Noguchi H, Yamauchi S, Tozawa Y, Ueda M, Hashimoto K, Koster P, Dong Q, Held K, Kudla J, Utsumi T, Uozumi N (2018) N-myristoylation and S-acylation are common modifications of $\text{Ca}^{(2+)}$ -regulated *Arabidopsis* kinases and are required for activation of the SLAC1 anion channel. *New Phytol* 218:1504–1521
- Shen J, Zhao Q, Wang X, Gao C, Zhu Y, Zeng Y, Jiang L (2018) A plant Bro1 domain protein BRAF regulates multivesicular body

- biogenesis and membrane protein homeostasis. *Nat Commun* 9:3784
- Shi H, Shen Q, Qi Y, Yan H, Nie H, Chen Y, Zhao T, Katagiri F, Tang D (2013) BR-SIGNALING KINASE1 physically associates with FLAGELLIN SENSING2 and regulates plant innate immunity in Arabidopsis. *Plant Cell* 25:1143–1157
- Shi S, Li S, Asim M, Mao J, Xu D, Ullah Z, Liu G, Wang Q, Liu H (2018) The Arabidopsis calcium-dependent protein kinases (CDPKs) and their roles in plant growth regulation and abiotic stress responses. *Int J Mol Sci* 19:1900
- Shinde SR, Maddika S (2018) Post translational modifications of Rab GTPases. *Small GTPases* 9:49–56
- Solis GP, Kazemzadeh A, Abrami L, Valnohova J, Alvarez C, van der Goot FG, Katanaev VL (2022) Local and substrate-specific S-palmitoylation determines subcellular localization of Galphao. *Nat Commun* 13:2072
- Sreeramulu S, Mostizky Y, Sunitha S, Shani E, Nahum H, Salomon D, Hayun LB, Gruetter C, Rauh D, Ori N, Sessa G (2013) BSKs are partially redundant positive regulators of brassinosteroid signaling in Arabidopsis. *Plant J* 74:905–919
- Stuhrwohldt N, Hartmann J, Dahlke RI, Oecking C, Sauter M (2014) The PSI family of nuclear proteins is required for growth in arabidopsis. *Plant Mol Biol* 86:289–302
- Su B, Wang A, Shan X (2022) The role of N-myristoylation in homeostasis of brassinosteroid signaling kinase 1. *Planta* 255:73
- Su B, Zhang X, Li L, Abbas S, Yu M, Cui Y, Baluska F, Hwang I, Shan X, Lin J (2021) Dynamic spatial reorganization of BSK1 complexes in the plasma membrane underpins signal-specific activation for growth and immunity. *Mol Plant* 14:588–603
- Tang RJ, Wang C, Li K, Luan S (2020) The CBL-CIPK calcium signaling network: unified paradigm from 20 years of discoveries. *Trends Plant Sci* 25:604–617
- Tang W, Kim TW, Oses-Prieto JA, Sun Y, Deng Z, Zhu S, Wang R, Burlingame AL, Wang ZY (2008) BSKs mediate signal transduction from the receptor kinase BRI1 in Arabidopsis. *Science* 321:557–560
- Thinon E, Serwa RA, Broncel M, Brannigan JA, Brassat U, Wright MH, Heal WP, Wilkinson AJ, Mann DJ, Tate EW (2014) Global profiling of co- and post-translationally N-myristoylated proteomes in human cells. *Nat Commun* 5:4919
- Towler DA, Adams SP, Eubanks SR, Towery DS, Jackson-Machelski E, Glaser L, Gordon JI (1987) Purification and characterization of yeast myristoyl CoA:protein N-myristoyltransferase. *Proc Natl Acad Sci U S A* 84:2708–2712
- Traverso JA, Giglione C, Meinnel T (2013) High-throughput profiling of N-myristoylation substrate specificity across species including pathogens. *Proteomics* 13:25–36
- Tsugama D, Liu S, Takano T (2012a) A putative myristoylated 2C-type protein phosphatase, PP2C74, interacts with SnRK1 in Arabidopsis. *FEBS Lett* 586:693–698
- Tsugama D, Liu H, Liu S, Takano T (2012b) Arabidopsis heterotrimeric G protein beta subunit interacts with a plasma membrane 2C-type protein phosphatase, PP2C52. *Biochim Biophys Acta* 1823:2254–2260
- Ueda T, Yamaguchi M, Uchimiya H, Nakano A (2001) Ara6, a plant-unique novel type Rab GTPase, functions in the endocytic pathway of Arabidopsis thaliana. *EMBO J* 20:4730–4741
- Vargova R, Wideman JG, Derelle R, Klimes V, Kahn RA, Dacks JB, Elias M (2021) A eukaryote-wide perspective on the diversity and evolution of the ARF GTPase protein family. *Genome Biol Evol* 13:evab157
- Wang C, Liu Y, Li SS, Han GZ (2015) Insights into the origin and evolution of the plant hormone signaling machinery. *Plant Physiol* 167:872–886
- Wilcox C, Hu JS, Olson EN (1987) Acylation of proteins with myristic acid occurs cotranslationally. *Science* 238:1275–1278
- Wu J, Tao Y, Zhang M, Howard MH, Gutteridge S, Ding J (2007) Crystal structures of *Saccharomyces cerevisiae* N-myristoyltransferase with bound myristoyl-CoA and inhibitors reveal the functional roles of the N-terminal region. *J Biol Chem* 282:22185–22194
- Xie Y, Zheng Y, Li H, Luo X, He Z, Cao S, Shi Y, Zhao Q, Xue Y, Zuo Z, Ren J (2016) GPS-Lipid: a robust tool for the prediction of multiple lipid modification sites. *Sci Rep* 6:28249
- Xiong WH, Qin M, Zhong H (2021) Myristoylation alone is sufficient for PKA catalytic subunits to associate with the plasma membrane to regulate neuronal functions. *Proc Natl Acad Sci USA* 118:e2021658118
- Xu J, Li HD, Chen LQ, Wang Y, Liu LL, He L, Wu WH (2006) A protein kinase, interacting with two calcineurin B-like proteins, regulates K⁺ transporter AKT1 in Arabidopsis. *Cell* 125:1347–1360
- Yamada M, Miki T, Goshima G (2016) Imaging Mitosis in the Moss *Physcomitrella patens*. *Methods Mol Biol* 1413:263–282
- Yamauchi S, Fusada N, Hayashi H, Utsumi T, Uozumi N, Endo Y, Tozawa Y (2010) The consensus motif for N-myristoylation of plant proteins in a wheat germ cell-free translation system. *FEBS J* 277:3596–3607
- Yi P, Goshima G (2020) Rho of Plants GTPases and cytoskeletal elements control nuclear positioning and asymmetric cell division during *Physcomitrella patens* branching. *Curr Biol* 30:2860–2868
- Zhang B, Wang X, Zhao Z, Wang R, Huang X, Zhu Y, Yuan L, Wang Y, Xu X, Burlingame AL, Gao Y, Sun Y, Tang W (2016a) OsBRI1 activates BR signaling by preventing binding between the TPR and Kinase domains of OsBSK3 via phosphorylation. *Plant Physiol* 170:1149–1161
- Zhang F, Li L, Jiao Z, Chen Y, Liu H, Chen X, Fu J, Wang G, Zheng J (2016b) Characterization of the calcineurin B-Like (CBL) gene family in maize and functional analysis of ZmCBL9 under abscisic acid and abiotic stress treatments. *Plant Sci* 253:118–129
- Zou JJ, Wei FJ, Wang C, Wu JJ, Ratnasekera D, Liu WX, Wu WH (2010) Arabidopsis calcium-dependent protein kinase CPK10 functions in abscisic acid- and Ca²⁺-mediated stomatal regulation in response to drought stress. *Plant Physiol* 154:1232–1243

Publisher's Note Springer Nature remains neutral with regard to jurisdictional claims in published maps and institutional affiliations.

Springer Nature or its licensor (e.g. a society or other partner) holds exclusive rights to this article under a publishing agreement with the author(s) or other rightsholder(s); author self-archiving of the accepted manuscript version of this article is solely governed by the terms of such publishing agreement and applicable law.

Figure S1. Sequence alignment of NMTs from selected eukaryotic lineages. Secondary structures are mapped according to the ScNMT1 structure (Bhatnagar et al., 1998). CoA, Ca, and Pe indicate residues that are involved in MyrCoA binding, catalysis and Gly2 recognition, and substrate peptide interaction according to HsNMT1 structure (Castrec et al., 2018).

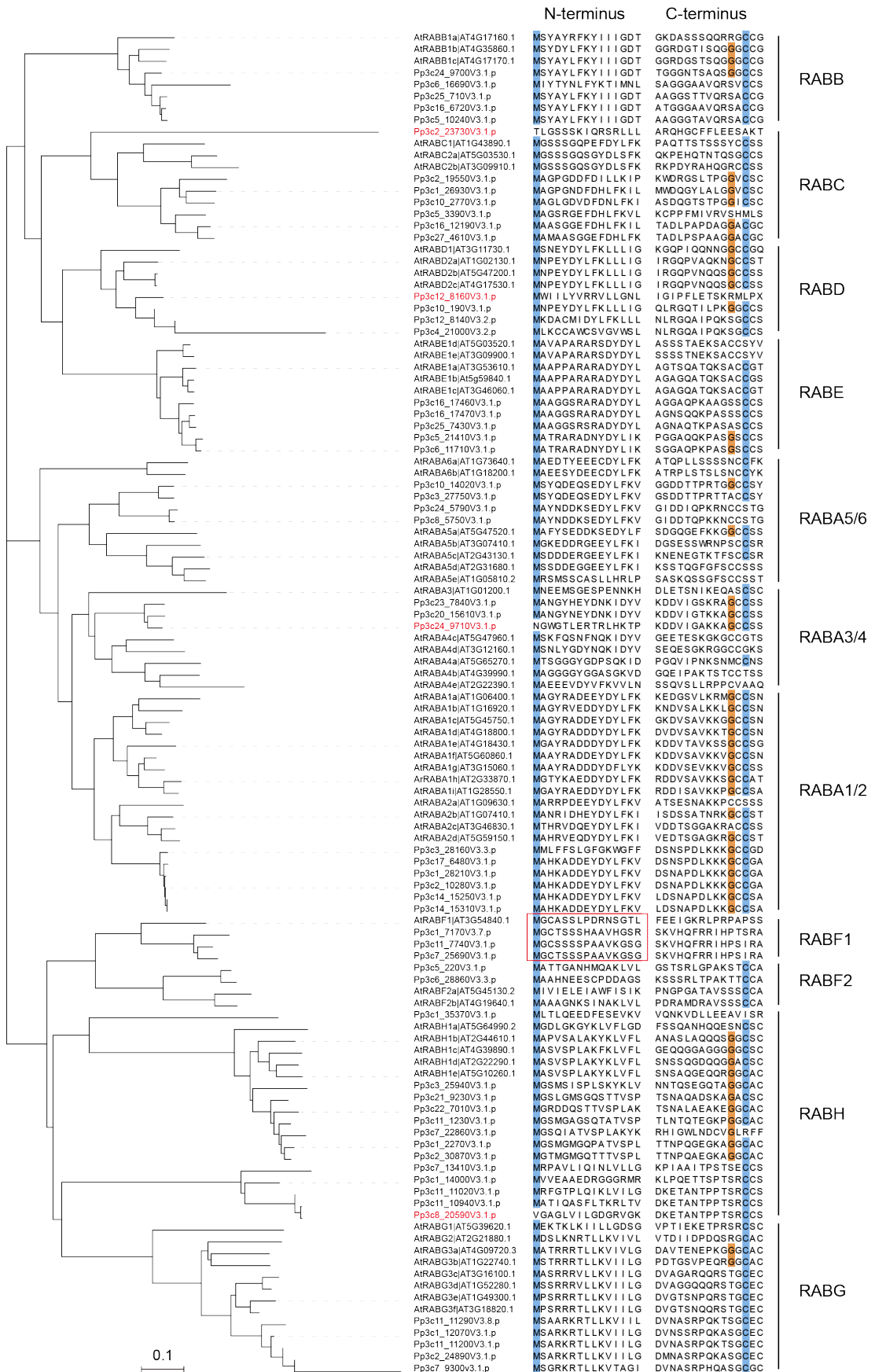


Figure S2. Phylogenetic tree and N-terminal sequences of Rab GTPases in *Arabidopsis* and *P. patens*.

The moss RABs are organized into ten groups. The majority of RABs have a prenylation signal (Cys-Cys or Cys-X-Cys) at the C-terminus. Only RABF1 contains a canonical dual lipid modification motif MGCXXXS (red box). The unaligned N-terminal and C-terminal 15aa of each protein are shown. Conserved residues are highlighted. Note that there are four genes (red IDs) whose sequences are incomplete in the Phytozome database.

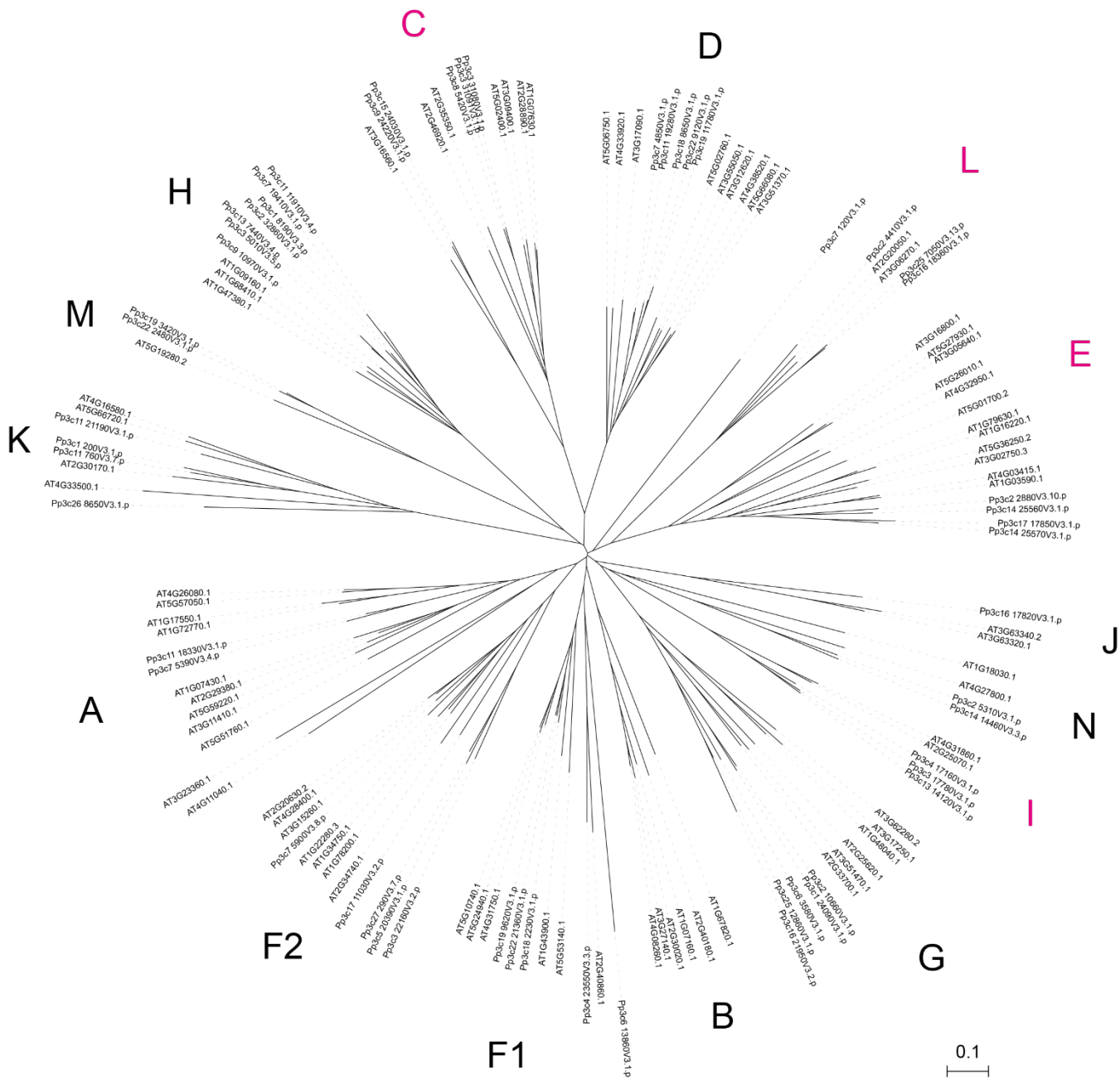


Figure S3. Phylogenetic tree of PP2Cs in *Arabidopsis* and *P. patens*.

The clades are named according to (Fuchs et al., 2013). Two additional clades M and N are defined in this study. The PP2C-I/C/E/L clades containing MYR substrates are shown in magenta.

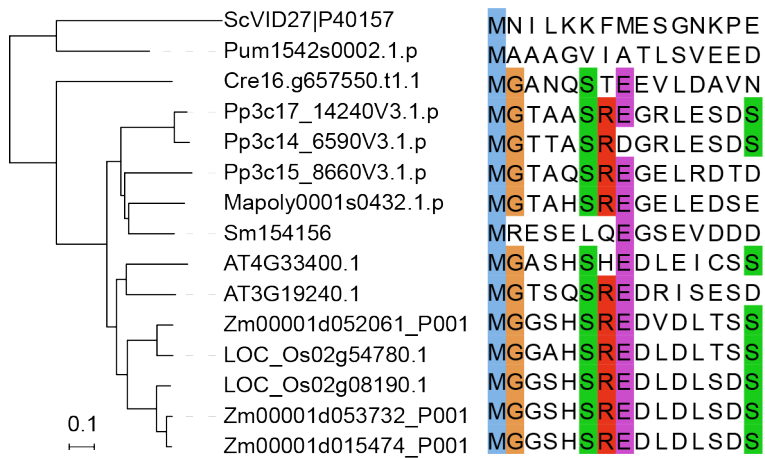


Figure S4. Phylogenetic tree and N-terminal sequences of VID27 domain-containing proteins.

VID27 domain-containing proteins have an MGGXXXSRE motif for MYR in green algae and land plants. This motif is absent in yeasts (ScVID27), red algae (Pum1542s0002.1.p), and the spikemoss *Selaginella moellendorffii* (Sm154156). Conserved residues are highlighted.

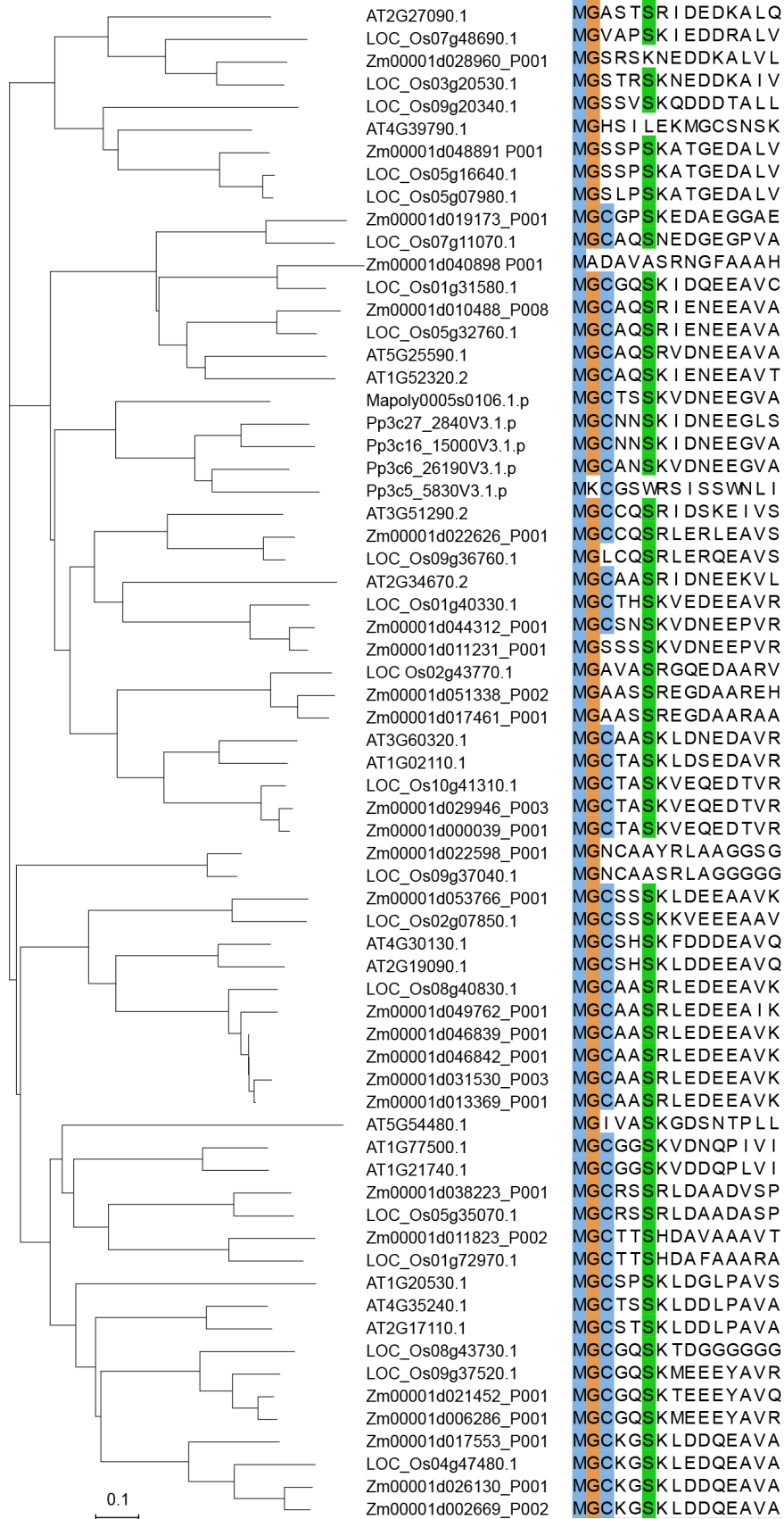


Figure S5. Phylogenetic tree and N-terminal sequences of DUF630 and DUF632 domain-containing proteins.

DUF630 and DUF632 domain-containing proteins are land plant-specific and have a highly conserved MGCXXS(R/K) motif for MYR in most members. Conserved residues are highlighted.